



**Trinity College Dublin**  
Coláiste na Tríonóide, Baile Átha Cliath  
The University of Dublin

# **Structural Health Monitoring of Wind Turbine Blades using Unmanned Air Vehicles**

by

**Smita Shivaram, B.Tech.**

**Dissertation**

Presented to the

University of Dublin, Trinity College

in partial fulfillment of the requirements

for the Degree of

**Master of Science in Computer Science**

**University of Dublin, Trinity College**

September 2015

# Declaration

I, the undersigned, declare that this work has not previously been submitted as an exercise for a degree at this, or any other University, and that unless otherwise stated, is my own work.

---

Smita Shivaram

August 27, 2015

## Permission to Lend and/or Copy

I, the undersigned, agree that Trinity College Library may lend or copy this thesis upon request.

---

Smita Shivaram

August 27, 2015

# Acknowledgments

Firstly, I would like to express my heartfelt gratitude to Dr. Ciarán Mc Goldrick, my supervisor and course director for his guidance, motivation, insightful contributions and patience throughout the course of my research. I would also like to thank my second reader and assistant supervisor Dr. Meriel Huggard for her valuable suggestions and encouragement. Besides my advisors, I would like to thank the technical staff of the School of Computer Science and Statistics(SCSS) for their timely assistance in procurement and configuration of hardware components.

I would like to thank my classmates and friends for all their help, suggestions and motivation throughout the course of my degree and research. Special thanks to Neil Savio Carvalho and Ayushmaan Kapoor for helping me out in times of need.

Finally, I would like to thank my father Shivaram Iyer for his encouragement, unwavering support and faith in my capabilities. I would also like to thank my family for their continuous support and enthusiasm.

SMITA SHIVARAM

*University of Dublin, Trinity College*

*September 2015*



# Structural Health Monitoring of Wind Turbine Blades using Unmanned Air Vehicles

Smita Shivaram, M.Sc.

University of Dublin, Trinity College, 2015

Supervisor: Ciarán Mc Goldrick

Structural Health Monitoring (SHM) is a key technique to ensure the health and safety of civil and mechanical structures. The most commonly used monitoring methods make use of a combination of techniques such as vibration-based methods, acoustic emission, thermal imaging and ultrasonic reflection in order to detect deformation or failure. The use of active image processing concepts in Structural Health Monitoring of static and moving civil structures is largely unexplored and presents an interesting area of research. The aim of this dissertation is to evaluate the use of visual imaging from unmanned aerial vehicles to autonomously monitor Wind Turbine blades in order to create a real - time model which can be used to assess its structural health. Early experiments and simulations provide promising results, and the use of powerful drones in combination with specialist software can be used to identify small-scale deformities. This opens up various potential areas of research such as 3D reconstruction of scenes and objects from Unmanned Aerial Vehicles, remote unobtrusive monitoring of moving mechanical structures using visual imaging and servoing etc.

# Contents

|  |           |
|--|-----------|
| <b>Acknowledgments</b>   | <b>iv</b> |
| <b>Abstract</b>  | <b>v</b>  |
| <b>List of Tables</b>  | <b>x</b>  |
| <b>List of Figures</b>   | <b>xi</b> |
| <b>Chapter 1 Introduction</b>  | <b>1</b>  |
| 1.1 Background . . . . .   | 2         |
| 1.2 Motivation . . . . .   | 2         |
| 1.3 Research Question . . . . .                                      | 3         |
| 1.4 Contributions . . . . .  | 3         |
| 1.5 Dissertation Structure . . . . .                                 | 4         |
| <b>Chapter 2 State of the Art</b>                                    | <b>5</b>  |
| 2.1 Structural Health Monitoring of Wind Turbines . . . . .          | 6         |
| 2.1.1 Wind Energy . . . . .  | 6         |
| 2.1.2 Overview of Wind Turbines . . . . .                            | 7         |
| 2.1.3 Structural and Condition Monitoring of Wind Turbines . . . . . | 8         |
| 2.2 Autonomous Control of Unmanned Air Vehicles . . . . .            | 12        |
| 2.2.1 Overview of Unmanned Air Vehicles . . . . .                    | 13        |
| 2.2.2 Flight and Control of Quadcopters . . . . .                    | 15        |

|                                 |   |           |
|---------------------------------|---|-----------|
| 2.2.3                           | Autonomous Drones . . . . .                           | 18        |
| 2.3                             | Visual Imaging and Servoing in Drones . . . . .       | 23        |
| 2.4                             | Structure from Motion . . . . .                       | 26        |
| 2.4.1                           | Feature Detection . . . . .                           | 28        |
| 2.4.2                           | Stereo Vision . . . . .                               | 30        |
| 2.5                             | Summary . . . . .                                     | 32        |
| <b>Chapter 3 Design</b>         |   | <b>34</b> |
| 3.1                             | Requirements . . . . .                                | 34        |
| 3.2                             | System Architecture . . . . .                         | 35        |
| 3.3                             | Learning Module . . . . .                             | 36        |
| 3.3.1                           | Drone pattern Estimation . . . . .                    | 37        |
| 3.3.2                           | Object Tracking . . . . .                             | 39        |
| 3.3.3                           | Distance Estimation . . . . .                         | 40        |
| 3.3.4                           | Correction Equation . . . . .                         | 40        |
| 3.4                             | 3D Reconstruction Module . . . . .                    | 42        |
| 3.4.1                           | Structure from Motion . . . . .                       | 42        |
| 3.5                             | Design Challenges . . . . .                           | 43        |
| 3.6                             | Summary . . . . .                                     | 45        |
| <b>Chapter 4 Implementation</b> |   | <b>46</b> |
| 4.1                             | Helical Path of the drone . . . . .                   | 46        |
| 4.1.1                           | Cartesian construction of helix . . . . .             | 46        |
| 4.1.2                           | Cartesian to Geographic Co-ordinates . . . . .        | 48        |
| 4.1.3                           | DJI GroundStation Waypoints API . . . . .             | 49        |
| 4.1.4                           | Summary . . . . .                                     | 50        |
| 4.2                             | Marker Tracking using Quadcopter . . . . .            | 50        |
| 4.2.1                           | Tracking motion using a colored marker . . . . .      | 51        |
| 4.2.2                           | Tracking differently colored moving objects . . . . . | 52        |

|                             |  |           |
|-----------------------------|--|-----------|
| 4.2.3                       | Sequential Differencing to identify motion . . . . . | 53        |
| 4.2.4                       | Summary . . . . .                                    | 54        |
| 4.3                         | 3D Reconstruction from 2D Image Set . . . . .        | 54        |
| 4.3.1                       | VisualSFM . . . . .                                  | 55        |
| 4.3.2                       | CMPMVS . . . . .                                     | 55        |
| 4.3.3                       | MeshLab . . . . .                                    | 56        |
| 4.3.4                       | Blender . . . . .                                    | 57        |
| 4.3.5                       | Summary . . . . .                                    | 57        |
| 4.4                         | Integration . . . . .                                | 57        |
| 4.5                         | Implementation Challenges . . . . .                  | 58        |
| 4.6                         | Overall Summary . . . . .                            | 59        |
| <b>Chapter 5 Evaluation</b> |  | <b>60</b> |
| 5.1                         | Rationale . . . . .                                  | 60        |
| 5.1.1                       | Factors . . . . .                                    | 60        |
| 5.1.2                       | Metrics . . . . .                                    | 61        |
| 5.2                         | Experiments . . . . .                                | 62        |
| 5.2.1                       | Experiment 1: . . . . .                              | 62        |
| 5.2.2                       | Experiment 2: . . . . .                              | 63        |
| 5.2.3                       | Experiment 3: . . . . .                              | 65        |
| 5.2.4                       | Experiment 4: . . . . .                              | 66        |
| 5.3                         | Summary . . . . .                                    | 67        |
| <b>Chapter 6 Conclusion</b> |  | <b>68</b> |
| 6.1                         | Research Questions . . . . .                         | 68        |
| 6.2                         | Conclusions . . . . .                                | 70        |
| 6.3                         | Future Work . . . . .                                | 71        |
| 6.4                         | Final Remarks . . . . .                              | 71        |

|  |           |
|--|-----------|
| <b>Appendix A Abbreviations</b>                            | <b>72</b> |
| <b>Appendix B DJI Phantom 2 Vision Plus Specifications</b> | <b>73</b> |
| <b>Bibliography</b>  | <b>74</b> |

# List of Tables

|     |   |    |
|-----|---|----|
| 2.1 | Power Output of wind turbines based on rotor size . . . . .               | 8  |
| 2.2 | Commercially available condition monitoring systems for wind turbines . . | 12 |
| 2.3 | Comparison of popular drones of 2015 . . . . .                            | 15 |
| 5.1 | Shortest Distance between drone and blade after linearization . . . . .   | 63 |
| 5.2 | Processing times for images of different resolutions . . . . .            | 66 |

# List of Figures

|      |  |    |
|------|--|----|
| 2.1  | Scope of system and corresponding areas of research . . . . .                              | 5  |
| 2.2  | Parts of a Wind Turbine[MHWF2015] . . . . .  | 7  |
| 2.3  | Increasing size of wind turbine blades[DNVGL2015] . . . . .                                | 7  |
| 2.4  | Yaw, Roll, Pitch and Uplift in a drone . . . . .   | 16 |
| 2.5  | X Configuration of Drone [Floreano2015] . . . . .  | 17 |
| 2.6  | + Configuration of Drone [Floreano2015] . . . . .  | 17 |
| 2.7  | Embedded Microcontroller on AR Parrot drone[Lugo2014] . . . . .                            | 20 |
| 2.8  | Structure of Remote Processing Station[Guimaraes2012] . . . . .                            | 20 |
| 2.9  | Design of Object Colour Tracking using Fuzzy Control [Olivares-Mendez2011]                 | 25 |
| 2.10 | 3D Reconstruction of a scene using SFM [Westoby2012] . . . . .                             | 27 |
| 2.11 | Key steps in the SIFT Algorithm . . . . .  | 29 |
| 2.12 | FAST Corner Detection[OpenCV2015] . . . . .  | 30 |
| 2.13 | 2D Stereo Vision[NI2015] . . . . .   | 30 |
| 2.14 | Multiview Stereo Vision[Westoby2012] . . . . .   | 31 |
| 3.1  | Simplified System Architecture . . . . .   | 36 |
| 3.2  | Architecture of the Learning Module . . . . .  | 37 |
| 3.3  | Identifying points on helix and conversion to real-world coordinates . . . .               | 38 |
| 3.4  | Difference between estimated and actual position due to wind and wake<br>effects . . . . . | 39 |
| 3.5  | Tracking two differently coloured spectral markers . . . . .                               | 41 |

|      |  |    |
|------|--|----|
| 3.6  | Steps in 3D Reconstruction Module . . . . .  | 42 |
| 3.7  | Object Estimation from Structure from Motion [Snavely2008] . . . . .                     | 43 |
| 3.8  | SFM Workflow . . . . .   | 44 |
| 3.9  | 3D Reconstruction using SFM . . . . .  | 44 |
| 4.1  | Algorithm for generating points on Helix . . . . .                                       | 47 |
| 4.2  | Processing Sketch to validate helix algorithm . . . . .                                  | 48 |
| 4.3  | Calculation of Helical Points around blade . . . . .                                     | 50 |
| 4.4  | HSV Image . . . . .  | 52 |
| 4.5  | Color Tracking . . . . .   | 52 |
| 4.6  | Longest contour . . . . .  | 52 |
| 4.7  | Pixel distance between two colored markers . . . . .                                     | 52 |
| 4.8  | Object tracking without color . . . . .  | 54 |
| 4.9  | Computation of SIFT points and perspective images in VisualSFM . . . . .                 | 56 |
| 4.10 | 3D point Cloud, Mesh and texture rendered using MeshLab . . . . .                        | 57 |
| 4.11 | Dense 3D Mesh rendered using Blender . . . . .   | 58 |
| 5.1  | Distance error in linearization of helix(Top View) . . . . .                             | 62 |
| 5.2  | Percentage error in distance of drone from blade due to linearization of helix . . . . . | 63 |
| 5.3  | Original Markers without blur . . . . .  | 64 |
| 5.4  | Markers with 13 % blur . . . . .   | 64 |
| 5.5  | Markers with 40 % blur . . . . .   | 64 |
| 5.6  | Markers with 60 % blur . . . . .   | 64 |
| 5.7  | Marker Detection Accuracy vs Percentage of Blur . . . . .                                | 65 |
| 5.8  | Time taken for 3D Reconstruction . . . . .   | 66 |



# Chapter 1

## Introduction

In recent years, wind energy has become a strong contender in the field of power generation. The rising prices and growing demand of non-renewable energy sources have sparked interest in clean, renewable sources of energy that can be harnessed effectively. Although wind energy has been used for small scale power generation in homes and farms for a long time in the form of traditional windmills, it is only in the last quarter of a century that commercial wind turbines have been used for large-scale electricity generation. As more countries increase their dependence on wind energy, turbine sizes have increased dramatically and many offshore and onshore wind farms have been constructed. Large scale wind turbines are quite expensive and have lifespans of upto 20 years. These turbines need to be constantly monitored for health and operating conditions, especially as they get older, as damage in the structure of the blade or failure can result in heavy monetary loss, environmental destruction and in some cases, even death.

This chapter first introduces the prior work done in the field of health monitoring of wind turbines from which the motivation of the dissertation is derived. Next, the objective of the dissertation is specified and a brief summary of the proposed approach is presented. The chapter concludes by outlining the structure of the dissertation along with a quick synopsis of each of the following chapters.

## 1.1 Background

The field of Structural and Condition Monitoring of wind turbines has been an active area of research over the last decade, and aims to improve safety and better understand operational loads and capacities of wind turbines. The most common methods in use today include vibration-based analysis, ultrasonic reflection, thermal imaging, principal component analysis, wavelet transforms and statistical monitoring. Most of these methods require physical sensors and actuator patches to be bonded to the surface of the turbine blade, which induces further strain in the blade resulting in damage or deformation. Some methods may also require that the blade be detached from the wind turbine before monitoring. Due to this, non-destructive monitoring techniques such as Acoustic Emission and Visual Imaging are being explored for suitability in this field. Approaches using Stereo Vision and Photogrammetry have been proposed, however, experimental tests indicate that further refinement is required before these methods can be used commercially.

## 1.2 Motivation

From the above section, it can be understood why unobtrusive monitoring mechanisms for civil structures are fast gaining popularity and do not cause damage by increasing load on the system. These methods also provide a more economically feasible approach as the cost of maintenance of wind turbines can be quite high, and normally ranges between 2 - 15 % of the cost of the wind turbine. Sophisticated image processing techniques are available today that can be effectively leveraged to solve the problem of Structural Health Monitoring. The advent of ubiquitous technology which provides enhanced capabilities such as flight and dynamic motion to cameras can also be used to address the gap caused by static positioning of imaging systems.

## 1.3 Research Question

The aim of this dissertation is to address difficulties in using computer vision techniques to perform health monitoring of rotating civil structures which cannot be effectively monitored through image or video obtained from a stationary camera. Based on the opportunity identified above, the following research questions has been posed:

*“Can visual imaging techniques be used to provide an efficient, unobtrusive and economical monitoring method for wind turbines?”*

This can be divided into further sub-questions as listed below:

1. What kind of image processing algorithm can be used for structural health monitoring of civil structures?
2. How can the algorithm be extended to be robust if the target structure is in motion and not stationary?
3. What are other factors which come into play while monitoring a wind turbine in realistic outdoor environments?
4. Can such a system be developed using commercial, easily available, off-the-shelf technology?

## 1.4 Contributions

The contribution of this dissertation is the design and implementation of a proof-of-concept system that uses a camera mounted on a quadcopter to follow a dynamic path around a wind turbine blade in order to accurately detect any damage, cracks or structural deformation in the blade. Such a system provides a significant contribution to the state of the art, as most of the research in this field considers the use of static or stationary visual sensors. Furthermore, such a system would perform autonomous monitoring with minimal human input. By integrating the elements of flight and dynamic motion with

a camera, many areas of potential research have been identified such as visual servoing around moving mechanical and civil structures, 3D reconstruction of scenes and objects for surveillance and monitoring etc.

## 1.5 Dissertation Structure

This section provides an outline of the structure of the thesis document.

- The current chapter provides a brief overview of the areas of research, gaps identified, research questions and contributions made by this dissertation.
- Chapter 2 divides the objective into specific areas of research. The state-of-the-art, background and related work for each of these areas are discussed in corresponding sections. A summary which connects all the areas of research and establishes their applicability to proposed system is presented towards the end of the chapter.
- Chapter 3 specifies the design aspects of the proposed system .The requirements of the system, the system architecture and component descriptions are discussed in this chapter. A quick synopsis of the design is presented at the end of the chapter.
- Chapter 4 discusses the methods & technologies used and challenges encountered while developing a system based on the design concepts described in the earlier sections. The specific libraries, programming tools and languages used are specified and a short summary of the implementation aspects is presented towards the end.
- Chapter 5 discusses the various metrics and factors used to evaluate the system along with experimental observations, and concludes with a quick summary of system performance.
- Chapter 6 provides answers to the research questions identified in Chapter 1, summarizes the contributions made by this research, lists future work and concludes with final remarks on the dissertation.

# Chapter 2

## State of the Art

The proposed system makes use of a variety of technologies such as drone automation, visual servoing, distance estimation from image and 3d reconstruction in order to achieve the required objective. This chapter reviews previous and ongoing research in four broad areas of research to examine the feasibility of our proposed system. This is represented in a diagrammatic notation in Fig 2.1. This chapter introduces the ongoing research in the

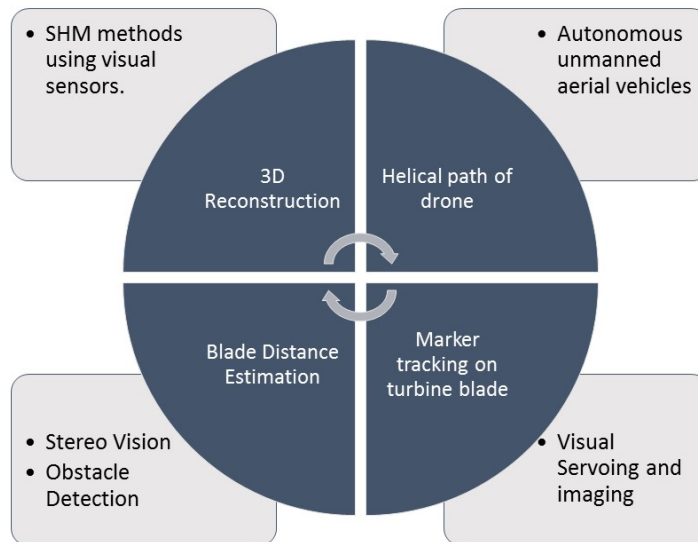


Figure 2.1: Scope of system and corresponding areas of research

different areas which comprise our project. Section 2.1 discusses the different techniques currently in use for the structural health and condition monitoring of wind turbines. We then examine various challenges faced and methods that have been suggested and deployed to overcome them. Section 2.2 introduces the reader to unmanned aerial vehicles, their flight, control & operation and reviews innovative technology that has been proposed to automate drone movements. Section 2.3 evaluates the use of visual servoing to control an unmanned aerial vehicle and Section 2.4 provides an explanation of the ‘Structure from Motion’ framework

## **2.1 Structural Health Monitoring of Wind Turbines**

This section presents methods in use, alternative approaches and ongoing research in the field of Structural Health Monitoring, specifically in the case of Wind Turbines. On reviewing the literature in this field, it is concluded that the most common commercially used Health monitoring methods use Modal Analysis, in which the vibrations of the wind turbine blades in motion are compared to its natural vibrating frequency to determine damage in the blade. The following sections provides an introduction to of wind energy, structure of a wind turbine, structural health monitoring methods and a short summary of the keypoints.

### **2.1.1 Wind Energy**

Wind Energy is emerging an integral source of power in many developed and developing countries. Since wind provides a clean and renewable option over other fossil fuel and is also available in plenty, many countries are looking to harness this form of energy efficiently to power both industries and homes. Due to decreasing costs, the market for wind energy has rapidly increased over the last two years and the global annual electricity production from wind farms has crossed the 390GW mark in 2014 [GWEC15]. Due to this demand, wind turbine sizes have been progressively increasing and large wind farms are

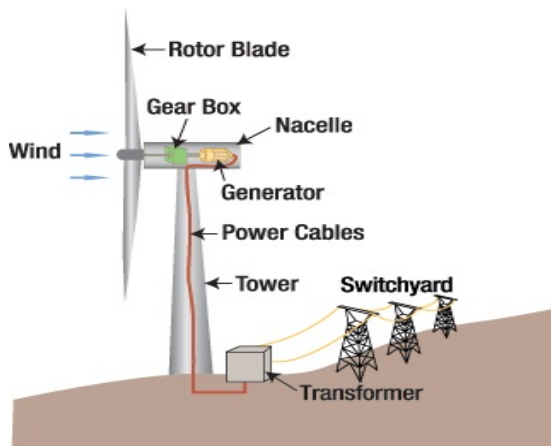


Figure 2.2: Parts of a Wind Turbine[MHWF2015]

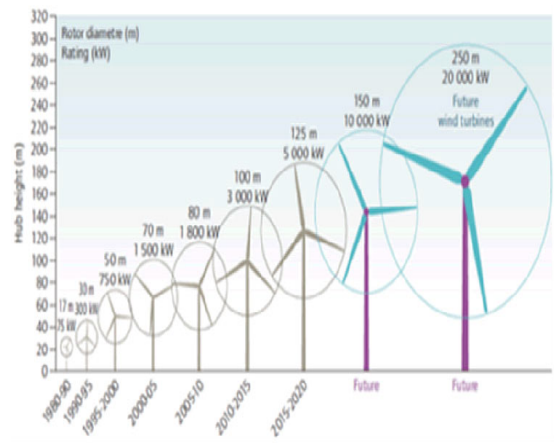


Figure 2.3: Increasing size of wind turbine blades[DNVGL2015]

being setup at offshore areas. The most commonly used commercial Wind Turbines have such as the GE 1.7MW model and 1.8MW Vestas V90 have blades with lengths over 70 metres which cover almost an acre of area during rotation[Veers2003]. A comparison of the size of turbine blades and power output produced is presented in Table 2.1[Layton2015]. According to the Global Wind Energy Council (GWEC) Statistics for the year 2014, China, USA and Germany are the biggest producers of wind energy at present.

### 2.1.2 Overview of Wind Turbines

A wind turbine consists of three blades which rotate about a central fulcrum called the hub. The hub is attached to the nacelle which houses the gearbox and other electrical and mechanical components. All of the above components are mounted on a tall steel tower. When wind blows, the blades rotate clockwise about the hub and the gearbox increases the speed of rotation and transmits it to the generator, which then converts it into electricity. For the blades to rotate efficiently, the turbine must be perpendicular to the direction of the blowing wind. For this purpose, a wind vane is used which points in the direction of the wind and the shaft of the blade is rotated about a yaw in order to turn the nacelle toward the wind [Hansen2008]. Based on the axis of rotation, wind turbines are classified into Horizontal Axis wind Turbines (HAWTs) or Vertical Axis Wind Turbines (VAWTs). Most

| Rotor Diameter and Maximum Power Output |                         |
|---|-------------------------|
| Rotor Diameter(in m)                    | Max power Output(in kW) |
| 10                                      | 25                      |
| 17                                      | 100                     |
| 27                                      | 225                     |
| 33                                      | 300                     |
| 40                                      | 400                     |
| 44                                      | 500                     |
| 48                                      | 750                     |
| 54                                      | 1000                    |
| 64                                      | 1500                    |
| 72                                      | 2000                    |
| 80                                      | 2500                    |

Table 2.1: Power Output of wind turbines based on rotor size

commercial large scale wind turbines are HAWTs, but newer wind farms use VAWTs as they collect wind from all directions and are hence more efficient.[Eriksson2008]. Modern wind turbines produce very little mechanical noise but produce large amounts of aerodynamic noise. This noise is known as ‘wake’[Adaramola2011]. In order to minimize the wake effect of one turbine on another in a wind farm, turbines must be spaced sufficiently far from one another as wake effects could prevent wind energy from being harnessed effectively.

### 2.1.3 Structural and Condition Monitoring of Wind Turbines

As the size of wind turbines increase, it is also crucial to ensure their safety as failure could be expensive and fatal. In addition to this, unscheduled maintenance of turbines is extremely expensive, and may cause unexpected downtime hence reducing the efficiency of wind farms. Maintenance may be corrective or preventive[Márquez]. Structural Monitoring can be used to estimate operational capacity, calculate blade fatigue and predict maintenance well in advance. Wind turbines are more susceptible to damage and failure compared to other civil structures because of acceleration fatigue caused by moving parts, and exposure to natural elements such as strong winds, rain, moisture in air and light-



ning[Ghoshal2000]. Most commercial wind turbines operate for about 120,000 hours over two decades during their lifetime. Maintenance costs are comparatively for new wind turbines but drastically increase as the turbine ages. The biggest wind turbine manufacturers such as GE, Vesta, Gamesa and Enercon spend approximately 1.5% to 2% of the wind turbine cost on its maintenance annually[Smead2014][WindMeasurementInternational2015].

## **Monitoring Methods**

Schubel *et al.*[Schubel2013] have presented a review on various Structural Health Monitoring techniques used in large wind turbine blades and describe acoustic, thermal, dielectric, ultrasonic and fibre-based approaches. The main aim of monitoring in wind turbine blades is to actively monitor the strain, load, fatigue and damage on the blades to prevent catastrophes and to gain better understanding of the operational loads of the turbine. Different monitoring methods are used based on whether the blades are stationary or in motion. The most common method in use today is based on vibration analysis. However, these methods require extra sensors and actuator patches to be bonded to the surface of the blade and increase load on the blade. Non-Destructive Testing(NDT) methods such as acoustic emission, ultrasonic reflection and imaging are an active area of research as they do not place further strain on the blade.

Ghoshal *et al.*[Ghoshal2000] published a review of different vibration-based techniques and compared four modal methods - Transmittance Functions, Operational Deflection Shapes, Resonant Comparison and Wave Propagation. Modal analysis works on the principle of comparing the resonant frequency of the blade in motion with its natural resonant frequency in order to identify defects. All the aforementioned methods have been explained mathematically along with measurement parameters. These damage detection techniques were applied to an 8-foot section of a fiberglass wind-turbine blade coated with retroreflective paint, and measured with a Scanning Laser Doppler Vibrometer (SLDV) placed at a distance of 15 feet, used to measure the vibrations induced by 6 piezoceramic

sensors bonded to the plate. Based on the tests conducted, it was concluded that Transmittance Functions were sensitive to both damage and noise obtained from the Frequency Response Function, and hence could detect but not localize damage. Operational Deflection and Resonant Comparison were shown to produce good response in realistic settings, however these techniques required further refinement to be used effectively. Wave Propagation was not able to detect damage which was outside the path between the sensor and the actuator and hence was unsuitable for use. One drawback of this paper is that the author claims that acoustic and visual methods for Structural Health Monitoring are not very effective without presenting any numerical or factual data to substantiate this claim.

Acoustic emission(AE) is quickly emerging as a non-destructive alternative to older methods. In this method, radiation of elastic waves is produced when there is any change in the internal structure of the object. These elastic waves are captured in an electric transducer and are then analysed to detect, localise and identify the kind of damage in the structure being monitored. AE can be used to detect various kinds of damage, such as fatigue cracks, structural deformities, delamination etc. However, most studies only focus on the relation between fatigue crack severity and emission produced but there is no complete solution which makes acoustic emission alone feasible for Structural Health Monitoring of mechanical structures[Rabiei2013][Bouzid2015][Grosse2008]. Recently, Dam *et al.*[Dam2015] have proposed a new method in which mechanical pencil breaks are used to produce acoustic emission from a blade which is captured by a piezoceramic sensor. Using a learning algorithm which teaches the system about emission frequencies, the sensors can be configured to detect damage in the blade.

In 2015, a new technique of fusing data from multiple Micro-Electro-Mechanical Systems(MEMS) sensors to identify and localize damage in the turbine blade was proposed by Moradi and Sivoththaman[Moradi2015]. This method is efficient due to its high accu-

racy and fast response. Two techniques of measuring strain using optimally placed sensors are presented by the authors —‘Perturbation Analysis’ and ‘Natural Frequency Analysis’. A fusion system for sensor validation and health diagnosis is created and applied to a blade of 33 metres. The strain in the system is simulated and the readings can be thresholded into four levels based on vibration and strain —Healthy, Damage Warning, Damage Blade Alarm (due to vibration frequency shift) and Damage Blade Alarm (both strain and vibration). The experimental simulations demonstrated successful results.

Yang *et al.*[Yang2010] introduce an electrical condition monitoring system as an inexpensive, efficient alternative to traditional SHM methods. Continuous Wavelet Transforms (CWT) are used instead of Discrete Wavelet Transforms(DWT) particular frequencies which are more efficient in signal analysis but computationally more expensive. Using power monitoring may have the disadvantage that the error in the power signal may not only be due to voltage or transducer error, but also due to the method of measurement used as well. The CWT adaptive filter is used to measure power signal in specific frequency bands, using a time-sliding frequency window. This approach was evaluated on a test rig in collaboration with Wind turbine manufacturers in simulated conditions with faults in synchronization and in the induction generator. The results showed that this was a feasible, inexpensive approach for condition monitoring of wind turbines. Some of the popular commercial Condition Monitoring products for wind turbines currently in use are listed in Table 2.2 [Crabtree2014].

A new unobtrusive monitoring technique makes use of virtual visual sensors in conjunction with a wireless sensor networks for fault detection. These include methods that make use of computer vision and image processing such as stereoscopic vision, Structure from Motion etc. whose use in the field of condition monitoring has not been explored in depth. Song *et al.*[Song2014] discuss the use of Virtual Visual Sensors to perform non destructive evaluation of wind turbines by using a continuous video input to determine

| <b>Product</b>      | <b>Manufacturer</b>  | <b>Monitoring Method</b>                         |
|---------------------|----------------------|--|
| Adapt WIND          | GE Energy            | Vibration , Oil Based                            |
| Brüel & Kjaer Vibro | Vestas               | Vibration, Acoustic, Sensor                      |
| CMS                 | Nordex               | Vibration  |
| CMaS                | Moventas             | Temperature, Vibration, Pressure                 |
| DCMS                | National Instruments | Vibration, Acoustic                              |
| OneProd Wind System | ACOEM                | Vibration, Acoustic, Thermal, Electrical Signals |
| SMP-8C              | Gamesa               | Vibration  |
| BLADEControl        | IGUS ITS GmBH        | Acceleration                                     |
| FS2500              | Fiber Sensing        | Fibre Optic                                      |
| SCAIME CMS          | SCAIME               | Temperature, Displacement, Tilt Sensing          |

Table 2.2: Commercially available condition monitoring systems for wind turbines

the modal properties of the blade while it rotates. The damage is detected and localized by analysing continuous wavelet patterns in the images obtained. This greatly simplifies the process of capturing and localizing defects in civil structures and also decreases the hardware infrastructure required. In the method of Stereo Vision, two cameras are placed at a fixed distance from each other to capture images of the structure from different angles. For moving objects, these cameras can be made to focus at particular points on the structure by applying spectral markers which guide the focus of the camera. Using the images obtained from both the cameras, a depth map is calculated which provides an idea of the three dimensional structure of the blade. The principle of Digital Image Correlation was applied to an industrial sized wind turbine blade and experimental results demonstrated that this approach could quantify and detect strain across the surface of the blade[LeBlanc2013].

## 2.2 Autonomous Control of Unmanned Air Vehicles

Unmanned Aerial Vehicles(UAVs) are flying vehicles that do not require an on-board pilot, and can be used to access remote or isolated areas. The use of such vehicles has opened

up many potential areas of research. Larger UAVs and aircrafts are generally used by the military for border patrol, testing nuclear weapons and launching missile systems at areas which are free from human civilization. Another kind of UAV which is garnering high amounts of interest in the last few years is the 'quadcopter' or drone. Quadcopters are much smaller than traditional UAVs and can be used in a number of civil and commercial applications. The scope of this literature review is restricted to quadcopters that can be used to monitor moving objects. The following sections provide an introduction to drones, their capabilities & uses, and autonomy of drones.

### **2.2.1 Overview of Unmanned Air Vehicles**

An Unmanned Aerial Vehicle (UAV) or Unmanned Aerial System(UAS) is an aircraft which does not require a human pilot on board, and can be controlled either remotely by a pilot or through an on-board computer system. Fully autonomous UAVs are subject to several legal and local regulations and are rarely used. Remotely monitored UAVs are used in both civil and military applications. A famous kind of UAV is the quadrotor or quadcopter. Quadcopters, used for industrial and commercial purposes, and are small aircrafts much like the joystick controlled helicopter toys, which can be controlled using a remote controller. The cost of drones are greatly decreasing with the advent of smaller and cheaper electrical components. They are widely used as a hobby by technology and flying enthusiasts. Drones can also be controlled semi-autonomously by automating simple path patterns through programming albeit with constant human monitoring. Drones are mostly mounted with lightweight cameras on a gimbal and are used for imaging and ranging applications. The usage of quadcopters is relatively new and needs to be dealt with caution as incorrect operation could cause failure and in rare cases injury.

The integration of drones in different fields will have huge social and economic impacts. Drones can form a middle layer between satellites used for imaging and human level imag-

ing. This will provide a mid-level view with sufficient detail which can be used for three dimensional scene reconstruction with high accuracy. They can be used in agriculture to monitor the growth of crops and to detect pest infestation. By mounting sensors on the drone, various kinds of surveillance activities can be carried out. They can also be used in the energy space to monitor the health of hydraulic turbines, wind turbines etc. However, one of the most important uses of drones will be in the field of e-commerce where they can be used to access remote areas that are not well connected by roads. By using drones that can lift small loads, delivery and return of ordered items can be facilitated quickly and efficiently. Coordination of automated drones can open up a lot more areas where UAVs can unobtrusively be used to improve everyday life. Incorporating terrestrial capabilities in drones in addition to its aerial capabilities can be greatly beneficial. This would allow drones to land & perch on walls or pillars and monitor from these vantage points without the need for constant hovering. This would help conserve the limited battery of the drone[Floreato2015].

## **Quadcopters**

A Quadrotor or Quadcopter is a specific kind of UAV , which is more commonly used in commercial applications. A quadcopter is a helicopter that makes use of four rotors instead of the conventional single blade rotor[Allen2015]. Quadcopters make use of four motors with attached propellers to create an upthrust that lifts the aircraft. Two of the motors rotate clockwise while the other two rotate counter-clockwise. Quadcopters are equipped with Vertical Take-Off and Landing ability(VTOL). These are much smaller than conventional UAVs and as a result, the battery life is greatly limited. Some of the most popular commercial drones today have flight times of slightly under 30 minutes. Quadcopters are fast gaining popularity because of their simplicity of use and maintenance[Hoffman2007]. They usually have four inputs and six outputs, and may be motorized or non-motorized[Hoffman2008]. The characteristic that differentiates quadcopters is their flying principle and the propulsion mode[Gupte2012]. All motions of

| Model                      | Camera       | Flight Time | Price Range |
|----------------------------|--------------|-------------|-------------|
| DJI Phantom 3 Professional | 12.4MP UHD   | 23 mins     | Expensive   |
| DJI Phantom 2 Vision Plus  | 14MP 1080 HD | 25 mins     | Expensive   |
| Parrot AR.Drone 2.0        | 720p HD      | 12 mins     | Mid-Range   |
| Hubsan X4 H107C 2.4        | 2MP HD       | 10 mins     | Economical  |

Table 2.3: Comparison of popular drones of 2015

the quadcopter can be obtained by varying 4 drone parameters. The quadcopter is made to fly by varying the throttle in the rotor. Some of the most popular and powerful quadcopters in use today are DJI Phantom 3, Hubsan X4 H107C 2.4 Quadcopter, DJI Phantom 2 Vision Plus, 3D Robotics Iris+ and Parrot AR. Drone 2.0 Power Edition [Baguley2015][TopTenReviews2015]. A brief comparison of some of these drones is presented in Table 2.3.

## 2.2.2 Flight and Control of Quadcopters

All motion and operations of the drone are controlled using four parameters —Yaw, Pitch, Roll and Uplift. ‘Yaw’ refers to the rotation of the head of the drone about the z-axis in a clockwise or counter-clockwise direction. ‘Roll’ flies the quadcopter sideways, either to left or right. ‘Pitch’ is the movement of quadcopter in the forward or backward direction while ‘Uplift’ increases or decreases the elevation of the quadcopter by increasing or decreasing thrust from the propeller blades. These four parameters are represented in Fig.2.4 shown below. To tilt the quadcopter along an axis, the throttles on one side are increased while that on the other side are decreased. To rotate the quadcopter, the rotation of the clockwise or counter clockwise rotors is increased. The quadcopter can be flown in two configurations the ‘X’ configuration and the ‘+’ configuration as shown in Fig 2.5 and Fig 2.6. The X configuration is generally more stable and easier to operate than the + configuration.

The algorithms used to control these devices can range from simple loop feedback to

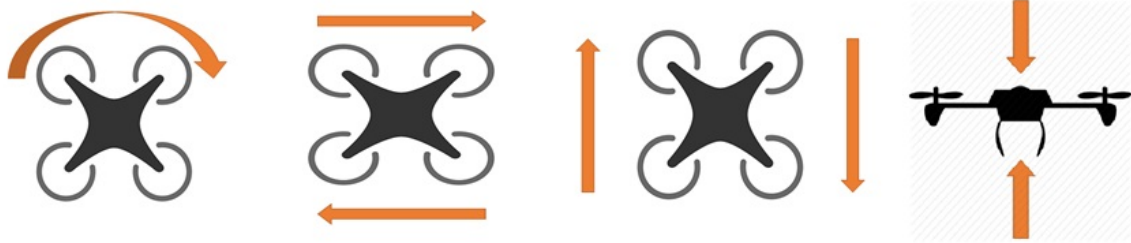


Figure 2.4: Yaw, Roll, Pitch and Uplift in a drone

complex neural networks. With the advent of low-cost and small sized sensors, the kinds and number of sensors that can be mounted on these devices is also steadily increasing. A quadrotor usually has some electronic controls and a microcontroller board, but may also contain a GPS and image processing software for camera motion estimation, obstacle detection etc. Control systems are used when multiple quadcopters need to collaborate on a task. Environmental challenges such as wind and terrain also play an important role in the flight of the drone. A good navigation system is essential for a quadcopter. These algorithms usually run on a remote computer and control signals are sent to the quadcopter. Testbeds are also being created to test these navigation algorithms efficiently and effectively.

Drones are flown singularly or as a swarm by developing a network between them. Swarm drones are used for border patrol, accurately tracking and localizing humans and objects. Ma'sum *et al.*[Ma'sum2013] developed a Particle Swarm Optimization (PSO) Algorithm in which each drone in the swarm would use its individual and global perception in order to recognize and track an object. This algorithm has been tested with both mobile and stationary targets.

### Safety Considerations

It is important to perform continuous monitoring of the drone while it is in flight as it may collide with a structure or bird and cause damage. Furthermore, in the presence of



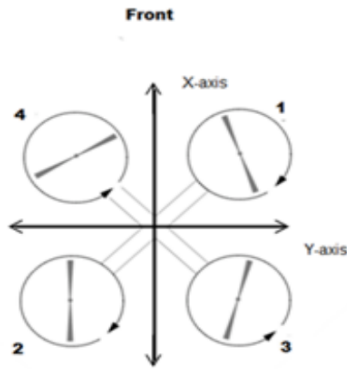


Figure 2.5: X Configuration of Drone [Floreano2015]

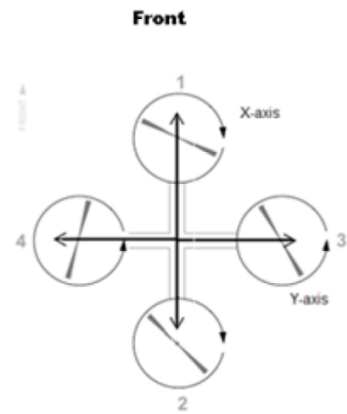


Figure 2.6: + Configuration of Drone [Floreano2015]

obstructions, drones may not perform well as they will not be able to lock on to GPS satellites. Drones are mostly used in three kinds of applications - recreational, civil or commercial, and military. Recreational drones are used as a hobby or for photography from unusual elevations or angles. Commercial Drones are used for surveillance, delivery of goods and terrain exploration. Military drones are used for Inspection, Surveillance and Reconnaissance (ISR) applications, unmanned killing, warfare and to test nuclear weapons [Wilson2014].

Murray & Park [Murray2013] highlighted the need for continuous monitoring of UAVs by human operators and propose a mathematical model through which autonomous movement and human monitoring & operation can be simultaneously balanced in order to improve safety and operation of UAVs. This article brings to light the importance of the human element in UAVs and the dangers of fully autonomous flight of such vehicles. The model suggested provides a new approach to determining amount and time of human input needed while flying a drone.

Wilson [Wilson2014] has presented a study of ethics in the usage of drones in various fields. A drone can be evaluated based on the person controlling them. There are three

levels based on which the drone's ethical component can be analysed:

1. The actions of the person controlling the drone
2. The intentions of the person controlling the drone
3. The consequences of the actions performed by the drone

Hence, in effect the moral framework is applied to the controller or end-user of the drone. A drone's ethics comes into play when its flight or operation causes hindrance to other people. This could include noise caused by the drone, invasion of privacy if people's pictures are captured without their permission or knowledge, stealth stalking etc. In commercial settings such as Amazon's AirPrime, a large number of drones may be used and hence cause crowding in the available airspace. This may inadvertently affect other flying manned vehicles by restricting the airspace available to them. They may also have negative environmental repercussions. From the military perspective, there may be a huge breach in ethics as collateral damage is likely. In unmanned killing through drones, there is a huge risk as wrong identification of target could result in the loss of an innocent life. Autonomy of drones is the most controversial as completely autonomy may cause a drone to misbehave during failure or error. Especially in critical military situations, excessive caution needs to be exercised.

### **2.2.3 Autonomous Drones**

One of the greatest advantage of drones is their capacity for autonomous flights in various environments. Due to this, their application in civil and industrial applications is ever increasing and no longer limited to military operations alone. New frameworks, methodologies and procedures are being developed to increase the reliability of autonomous drones. Today, technological advances have reached a sufficiently mature level where drones can be flown semi-autonomously. However, at present, the commercial drones available are inaccurate to use at ground level or inside closed spaces and may misbehave due to lack of

control signals. Due to this, the full potential of autonomous drones cannot be achieved as some amount of user supervision is necessary[Floreano2015].

### **Autonomy in drones**

Autonomy in robots is the ability of robots to function by themselves without manual input, by maintaining knowledge of state and using some sensing techniques. Autonomy frees the drone from human supervision and increases scope of use. There are different increasing levels of autonomy that a drone can have which are listed below[Floreano2015]:

- **Sensory-motor autonomy:** This translates high-level commands to the drone such as to fly to a particular height, move to a GPS point etc. into low-level platform-specific combination of yaw, roll and pitch.
- **Reactive autonomy:** This is built over sensory-motor autonomy. In this kind of autonomy, the drone maintains its position even in the presence of wind, signal failure and other unpredicted occurrences. It also helps the drone avoid obstacles in its path and maintain a fixed distance from a stationary or moving object.
- **Cognitive autonomy:** This built over both reactive and cognitive autonomy. This is used to perform complex operations such as object recognition and tracking, mapping and localization.

A drone with Cognitive autonomy is completely exempt from human supervision. The drone uses incoming data and state information at a point to determine its future action. Reactive autonomy requires minimal supervision while sensory motor autonomy requires moderate human supervision.

Mellinger *et al.*[Mellinger2011] developed a drone system which made use of cognitive autonomy to fly through windows, perch on walls or wires and to follow aggressive trajectories. Multiple-drone systems were programmed to achieve cooperation in manipulating

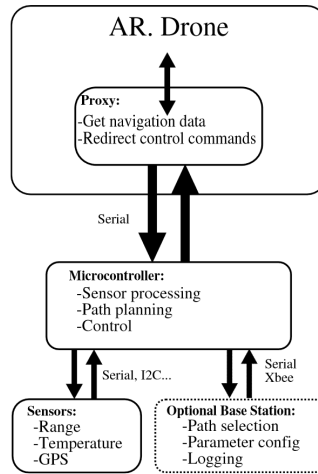


Figure 2.7: Embedded Microcontroller on AR Parrot drone[Lugo2014]

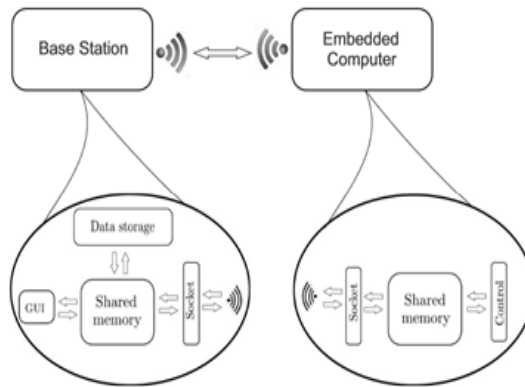


Figure 2.8: Structure of Remote Processing Station[Guimaraes2012]

a payload through rigid attachments. A gripper system was also developed to enable robot climbing. The experimental results showed that autonomous behaviour was possible for singular and multiple drone systems. Autonomous drones usually make use of an on-board computer system or a remote base station for processing input and correct navigation of the drone. This is shown in Figure 2.7 and Figure 2.8

Chen *et al.*[Chen2013] proposed the design for a spatially aware autonomous drone using a quadcopter, an Android phone or tablet, an Arduino microcontroller and ultrasonic sensors that could be used to autonomously navigate the drone to explore a new loca-

tion. Such a system would be highly useful in the field of Intelligence, Surveillance and Reconnaissance(ISR) for wars, border surveillance and exploring unmanned areas including search and rescue. The system is constructed in three parts - setting up the system hardware, establishing the navigation and control within indoor locations and inferring the position of drone and its surroundings from images. The Arduino-Android interface was found to be highly complex and caused flight instability. The experimental results indicated that such a system was highly feasible and could be extended and refined to commercial drones. A similar system with improvements was suggested by Chirtel *et al.*[Chirtel2015] which could be used to construct the map of an unknown indoor space. A Simultaneous Localization and Mapping(SLAM) framework was incorporated to create a map of the location autonomously. This system is designed using Commercial Off-the-Shelf(COTS) technology in order to use economical equipment and evaluate the ease of developing such a system. An android phone is mounted on the quadcopter and communicates with a mounted input output board(IOIO) through Lidar. The experimental results indicated that the lack of GPS signal made it difficult for the drone to hold its position and avoid obstacles, and hence such a method is not very effective.

An effective prototype for a fully autonomous quadcopter was proposed by Guimaraes and team in 2012 [Guimaraes2012]. In this design, a master-slave architecture is used where an embedded microcontroller acts as the designated master. The data obtained from the drone is processed at the radio base station which offers significant advantages in comparison with on-board processing. This is represented in Fig 2.8. As the computing power on board is very limited due to the size of the drone, complex operations may take too much time to process or may not be feasible at all. Furthermore, intensive operation will drain the battery of the drone thereby greatly decreasing the flight time of the system. A stabilization strategy is used in conjunction with the algorithm in order to maintain the drone's orientation while varying the Yaw, Pitch and Roll parameters. A simulation testbed for this system was developed using Matlab and PID Controllers. The findings

from this experiment indicated that this system performed well even in the presence of noise. Lugo & Zell proposed a similar system using the AR Parrot drone. The vertical orientation of camera and detected FAST corners are used to maintain position of the drone and vary its horizontal velocity. A second algorithm that uses pyramidal images and computes optical flow is used for accuracy. An on-board embedded microcontroller is present which processes the incoming input and controls motion and navigation of the drone.

Various other approaches to automate drones have been proposed in recent times. All of these make use of some imaging or ranging technique along with a stabilization strategy. Jang *et al.* suggested the use of MEMS sensors and Kalman Filters in order to make accurate estimations even in the presence of noise [Jang2007]. A Four Stroke RC Engine was used with a quadcopter to test autonomous flight [Bluteau2006]. The RC engine is primarily used to increase the power to weight ratio of the quadcopter. A distributed software and hardware architecture was used in the setup of the system. Two kinds of sensors are mounted on the drone - proprioceptive sensors for low-level commands and exteroceptive sensors for high-level commands. Results indicate that further refinement of this design is required for 3d localization. Methods using acoustic emission and reflection have been explored but results and simulations indicate that these are not very effective. Based on the literature review, the best algorithms to autonomously move the drone in an indoor or a non GPS-accessible location by producing a location map use ultrasonic reflection and visual imaging. Simple and complex image processing algorithms such as Stereo Vision, Feature detection, template matching and servoing techniques have been implemented and tested by various teams. A detailed description of some of these imaging techniques and experimental simulations have been described in the following section.

## 2.3 Visual Imaging and Servoing in Drones

As most commercial drones are mounted with good quality cameras, they can use visual techniques in order to track and detect objects. Vision-based navigation and tracking has become a very important aspect in the field of robotics. This approach can not only be used to capture images of objects or scenes but also to detect moving objects, follow objects at fixed distances, provide localization, estimate paths and monitor risky areas. Camera operations and computer vision applications form the largest area in which drones are being commercially used today. Visual Servoing is the process of using visual input to control the movement of the drone such as tracking a particular template, colour, shape etc. This can be done in two ways in an Unmanned Aerial Vehicle - by either moving the quadcopter at a fixed distance from the moving object, or by keeping the quadcopter stationary and focusing the camera on the object as it moves.

Achtelik[Achtelink2009] presents the prototype of a system in which the motion of a quadcopter is controlled through visual feedback and inertial sensors. Well-designed markers are used for easy detection, and to facilitate robust movement in the presence of noise. The quadcopter has an Inertial Measurement Unit(IMU) consisting of accelerometers, gyroscopes and two processors of which one is used to communicate to a base station wirelessly. Small, inexpensive VGA cameras were mounted on the quadcopter and the maximum distance to detect a marker was established as 5 meters. Four markers (strong LEDs within ping pong balls) were used to reduce exposure time of the camera in order to avoid motion blur and ambient light. For tracking and reconstruction, the centre of gravity is calculated for each of the markers by transforming the RGB plane into a YUV plane, and applying a median filter to determine its correct centre in neighbourhood. The 3D coordinate centres are then obtained from the 2D centres and used to determine the quadcopter's position and orientation. The processing times and delays were measured before control with the help of initial inertial sensors. The system was evaluated based

on stability of the drone while stationary and in motion and was reliable in tracking the quadcopter.

An interesting approach and control strategy to follow the path of a 3D moving object using an unmanned air vehicle (UAV) is presented by Mondragón *et al.*[Mondragón2011]. This method uses visual data input and performs colour distribution based segmentation in order to develop an Image-based Visual Servoing system. The UAV maintains a fixed distance from the centre of the moving object and from the image plane in order to ensure stable motion and continuous detection. This approach is tested in indoor as well as outdoor settings. Detection of the moving object through camera input is difficult because it is susceptible to sudden changes in illumination and color. For initial object detection, the author has proposed a simple colour distribution based extraction. For Visual Servoing, it is ensured that the target is present in cameras field of vision and at a fixed distance from the UAV. Based on the results obtained, it is concluded that such an approach is feasible and also robust to environmental conditions.

Visual Servoing systems are classified into two categories:

- Pose-based: Using pose estimation
- Image-based: Using image information

Hamel & Mahony proposed an image-based navigation strategy for drones[Hamel2005] which makes use of pose particle information to calculate the visual error. A decoupled control design using structured control Lyapunov function is implemented in this system. The experimental simulation for this system is conducted with a an X4-flyer drone and demonstrates that the control functions effectively in 2D. An improvement to the aforementioned system is proposed by the authors to increase the system's efficiency[Guenard2008]. A non-homogeneous gain term is added and adapted to the error measurements in order to balance out the poor conditioning of the image Jacobian matrix.



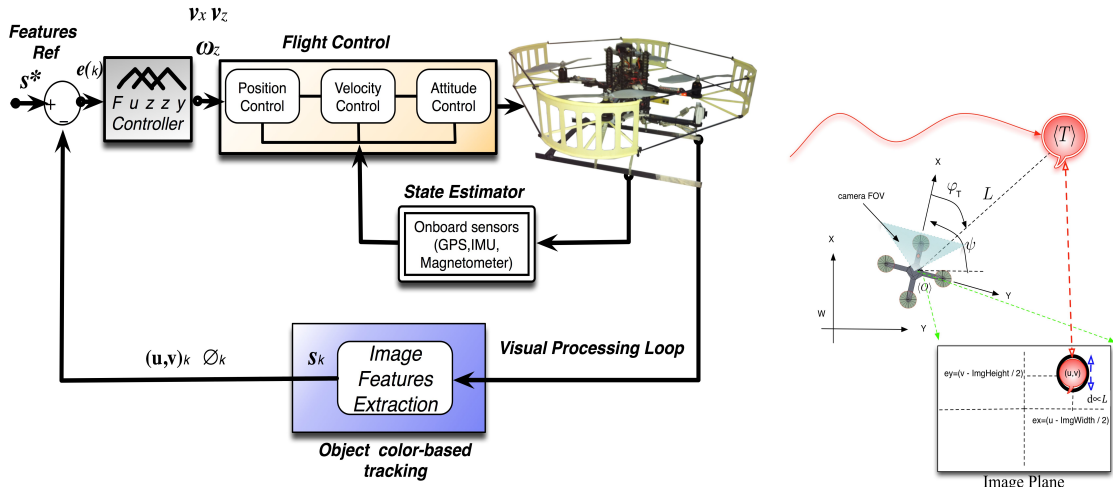


Figure 2.9: Design of Object Colour Tracking using Fuzzy Control [Olivares-Mendez2011]

The results exhibit the robustness and efficiency of this algorithm.

Ian Golightly and Dewi Jones have explored the use of unmanned aerial vehicles for inspection and monitoring of overhead power lines [Golightly2005]. The quadrotor would draw electricity from these wires which would offer significant advantages over a freely flying drone. Hough Transform is used to obtain the position and orientation (pose) information from the UAV. The experimental tests are conducted in lab and the results show that such a system is useful, accurate and resistant to noise and disturbances.

Vision4UAV is a software that provides vision based capabilities to Unmanned Aerial Vehicles such as Object Detection, Localization and Tracking using Fuzzy Servoing [Olivares-Mendez2011]. The camera mounted on the rotary wing of the drone focuses on continuously following an moving target object in air, and maintaining a fixed distance from it. This algorithm is tested on real flights in various scenarios and is validated to be robust to changes in wind, illumination and perturbation. This system can also be used for swarm flying in formation and for indoor navigation. The design of this system is represented in Fig 2.9. A similar design will be used in the proposed system.

## 2.4 Structure from Motion

Structure from Motion(SFM) is a 3D reconstruction framework based on the principle of photogrammetry. Photogrammetry is used to estimate measurements and depth from 2D images and also for accurately determining surface points in an image. It makes use of ultrasonic reflection to estimate 3D motion in a reference field. SFM is fast growing as an area of interest as it can be used to construct 3D models of scenes or objects from a set of 2D images without a 3D correspondence input parameter. In simpler words, SFM is the automatic recovery of camera motion and scene from a set of images. SFM is used in various computer vision applications such as shape reconstruction, navigation & tracking and in generation of Computer Generated Imagery (CGI).

3D reconstruction of a scene can take place in one of two ways. In the first method, some prior knowledge of the scene is used in order to make estimations and increase the degrees of freedom. For example, the use of a planarity constraint can give some idea regarding the positions of points from an image to 3D space. The second method suggests use of corresponding image points like Corners or Edges in multiple views. Using different views of an image, a 3D point can be reconstructed by 'triangulation'. Camera calibration, position and orientation need to be determined and expressed using a projection matrix. The 3D model is constructed by determining and matching the same feature in different views[Szeliski2011]. Structure from Motion is mainly based on two major principles - Feature Extraction and Stereo Vision. Various algorithms have been developed for research on SFM. The two most popular frameworks are the Stanford 'Bundler' algorithm and the 'VisualSFM' framework. Both of these can be used for research and lab purposes but do not produce very accurate results in comparison with specialist software.

Pollefys suggested a similar method for the reconstruction of 3D scenes from 2D images[Pollefys05]. The motion and calibration of the camera and the shape of a rigid static



Figure 2.10: 3D Reconstruction of a scene using SFM [Westoby2012]

object being photographed can be recovered from an image sequence. The approach presented was fully automatic and could handle photo or video sequences acquired with uncalibrated hand-held cameras. A much more refined algorithm was presented by the author for real-time 3D reconstruction of urban scenes [Pollefy2008]. Instead of using individual images, a video stream is taken as the input along with GPS and inertial measurements so that the reconstructed model can be placed in its estimated geographic co-ordinates. Accuracy is achieved by using a two-step stereo reconstruction process and exploiting the redundancy across frames. Results are tested on video sequences comprising hundreds of thousands of frames.

A fully automated 3D reconstruction and visualization system is suggested for buildings and architectural scenes by Furukawa and team [Furukawa2009]. This method claims to be applicable to both interior and exterior environments. This presents a challenging problem as it is difficult to reconstruct walls as they have no markers or textures to perform keypoint matching. The system makes use of structure from motion, multi-view stereo and stereo vision in order to calibrate camera and recover the 3d geometry of the objects in the scene. Depth-maps are used in order to compute simplified real world models. Finally, the model is rendered in an image-based 3d viewer. Using this algorithm, the 3d model of the entire first floor of a house was produced.

### 2.4.1 Feature Detection

Features are interesting points in an image that can be used for low-level processing operations. During feature detection in an image, each and every pixel is examined to see if it contains a feature. In this manner, all the feature pixels in an image are extracted and used for various kinds of operations. Some common features include edges, corners and blobs. Many sophisticated feature detection algorithms use SIFT feature detection or FAST Corner detection which are described in the following sections.

#### SIFT Feature Detection

Scale Invariant Feature Transform (SIFT) is a feature detection and extraction algorithm that was proposed by David Lowe in 1999. SIFT has gained popularity because of its robustness to illumination changes, scaling, noise, affine distortion and rotation. In this algorithm, a training image is provided to the algorithm from which features are extracted. These features are then stored in a database. An object in a test image is detected by comparing the features in the database to the features in the test image based on the Euclidean distance between its feature vectors. From the set of matches, few are discarded and the good ones are maintained. Objects which pass these matches are identified and then extracted. The SIFT algorithm can be broken down into 5 steps which are described below[Lowe1999]:

1. **Scale-Space Extrema Detection:** Difference of Gaussians(DoG) is calculated for the image with blurring of the image with scaling parameters  $\sigma$  and  $k\sigma$ . Using the DoG, images are searched for local extrema over scale and space, i.e, each pixel is compared with its neighbours in the current scale and its previous and next scale. If it is the local extreme in its neighbourhood, it becomes a potential keypoint.
2. **Keypoint Localization and Filtering:** The keypoints are then filtered to obtain accurate results. Taylor Series Expansion of Scale is used to check if the extrema is lesser than the threshold. If the extrema is lower than the threshold., it is discarded.

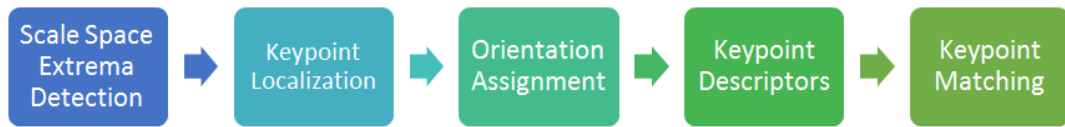


Figure 2.11: Key steps in the SIFT Algorithm

This removes all the low-contrast points and maintains strong keypoints.

3. **Orientation Assignment:** Orientation is assigned to each of the keypoints in order to make it rotation-variant. A scale-dependent neighbourhood of each of these points is considered and the gradient and direction is calculated. This creates keypoints with same location and scale but with different orientations. All of these
4. **Keypoint Descriptor:** A 16x16 neighbourhood around the keypoint is divided into 16 sub-blocks of 4x4 size. An 8-bin orientation histogram is created for each sub-block. The bin is represented as a vector to form a keypoint descriptor.
5. **Keypoint Matching:** Keypoints in two images are matched by examining their corresponding neighbours.

Various improvements have been proposed to the SIFT algorithm such as -SIFT, N-SIFT, PCA-SIFT and Color SIFT by extending scale and dimension in order to improve the speed and accuracy of matching. SIFT is being widely used in medical imaging, image registration, identifying unknown areas and robotic mapping and navigation.

### **FAST Corner Detection**

Features from Accelerated Segment Test (FAST) was developed by Edward Rosten and Tom Drummond, is used for feature detection & extraction and can be used for tracking objects in scenes. It is primarily used to identify corner points in an image. The FAST algorithm is much faster than other feature detection algorithms such as SIFT and Harris-

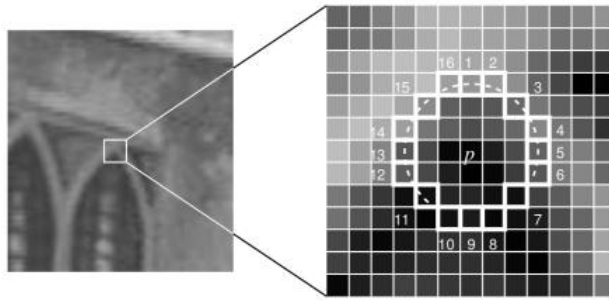


Figure 2.12: FAST Corner Detection[OpenCV2015]

Plessey Corner Detection. For each pixel, the 16 pixels on the circle of radius 3 around the point are considered. If 'N' of these surrounding pixels are greater than the pixel intensity plus a threshold value or lesser than the pixel intensity minus a threshold, then the point is identified as a corner. The threshold value and the value of 'N' are obtained through machine learning.

## 2.4.2 Stereo Vision

Stereo Vision is the process of estimating 3D information from a set of cameras which capture images from different angles or perspectives. This is obtained by examining relative positions of the same object in different images. Stereo Vision is generally used for creating depth maps of an object by following some assumptions like planarity or linearity. In the most basic, form, stereo vision makes use of 2 different cameras placed

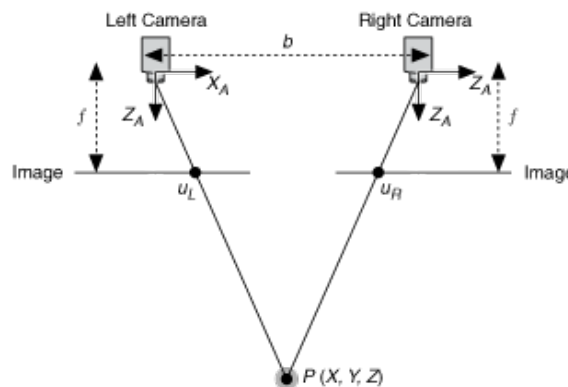


Figure 2.13: 2D Stereo Vision[Ni2015]

at a fixed vertical or horizontal distance from each other. This produces two views of

the same scene. From these views, relative depth estimations can be obtained. This is done using the principle of *triangulation* where, an object's distance from the camera can be obtained using 3 parameters namely dimension (height or width of the object being captured), pixels that it occupies in the image and focal length of the camera. Using this technique, the actual distance between two points can be computed. Camera calibration is a very important step in stereo vision in order to determine focal length of the camera and also account for distortion in image.

Multi-view Stereo Vision makes use of several views from an object to compute distance between various points or markers on the surface of an object. The camera is moved around the object in a circle and using the different depth maps obtained, a 3d point cloud can be constructed. A representation of Multi-view Stereo Vision is depicted in Fig 2.14. Multi-view stereo vision forms the basis for the Structure-From-Motion Framework. Stereo Vision has reached a level of maturity where the algorithm has been used in vari-

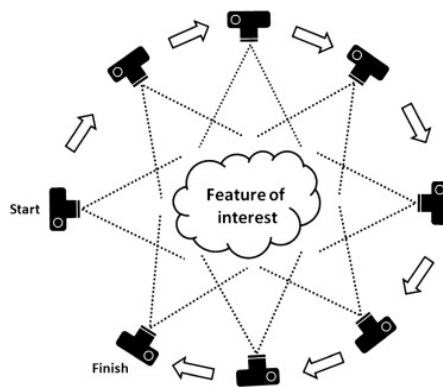


Figure 2.14: Multiview Stereo Vision[Westoby2012]

ous critical applications such as planetary exploration and outer space navigation [Goldberg2002]. The use of robotic stereo vision forms the fundamental basis of autonomous robots and has been applied to various situations like UAV automation, robotic tracking, road traffic surveillance and monitoring, border patrol etc. One of the most famous applications of this method is the self-driving car. Stereo vision is also used for SLAM applications to build grid maps of unknown areas or environments. Various techniques

have been proposed to reduce the disparity in the map information obtained from stereo vision. Don Murray[Murray2013] proposed a methodology through which the errors created by occupancy grid mapping can be overcome successfully. Errors are reduced by using continuous disparity surfaces to separate and classify images based on the “spikes” caused by mismatches.

Through the use of SIFT and multi-view stereo vision, a 3D model can be obtained. This combined algorithm constitutes the SFM framework.

## 2.5 Summary

Over the last quarter century, there has been a tremendous growth in the field of wind energy. Traditional windmills located at the farms and houses have given way to large-scale wind turbines whose blades are more than 65 metres in length. As these large blades move continuously and are exposed to natural elements like wind, rain and lightning, there is a crucial need to monitor them continuously in order to prevent failure which could cause heavy monetary loss, damage and even death. Various wind turbine monitoring mechanisms are used such as Vibration-based analysis, Ultrasonic reflections(Sonar, Lidar), thermal imaging and oil-based methods. Most methods require some physical sensors to be bonded to the surface of the wind turbine blade and hence, induce further strain in the blade. Non-destructive, unobtrusive methods such as Acoustic emission and Visual Imaging are gaining popularity and have become popular areas of research in the field of Structural Health Monitoring. The proposed system explores the use of computer vision algorithms for monitoring wind turbines.

Unmanned Aerial Vehicles(UAVs) or drones have moved from being military equipment and are now being widely used in civil and commercial areas. Due to their small size and flight capability, quadcopters have become extremely popular as they provide ”eyes-in-the-



sky”. One of their greatest uses today is Simultaneous Localization and Mapping(SLAM) applications where they can be used to create grid maps of unknown or unmanned areas. This greatly improves safety of critical applications. They are also used for surveillance and monitoring of traffic, for three-dimensional reconstruction of scenes and for border patrol. The numerous advantages offered by commercial-off-the-shelf drones can be harnessed effectively to monitor civil structures. In the case of civil structures in motion, flight in different patterns around these structures can allow for closer unmanned inspection. As most commercial drones today are fitted with a high definition camera, visual imaging capabilities can be leveraged over the mobility of the drone to perform effective monitoring. This aspect forms a key element of the proposed system.

With growing advances in the field of image processing and computer vision, small amounts of detail in a scene can be calculated using different methods. 3D reconstruction of objects and scenes has become a huge area of research and has uses in medical imaging, geographic applications such as surveillance and mapping, and in almost all fields of animation. If 3D reconstruction can be used in the field of Structural Health Monitoring by obtaining models of sufficient detail where damage, strain or deformation can be detected, it can be widely used as economical and feasible alternative to traditional monitoring methods. Structure from Motion or Stereo Vision can make use of different views taken from a camera for 3D reconstruction of the scene. From the research, it can be concluded that one novel approach to SHM could be by making use of unmanned aerial vehicles mounted with visual sensors in order to construct a real-time, 3D model from a 2D image set in order to detect damage or failure in the structure.

# Chapter 3

## Design

This chapter specifies the design aspects of the proposed system. First, the requirements of the system are listed to provide a thorough understanding of the objective of the dissertation research. Next, the proposed system architecture is presented followed by detailed descriptions of each of the system's components. Finally, a quick summary of the design pattern, principles and techniques used is presented to the reader.

### 3.1 Requirements

A preliminary analysis of the objectives of our system reveal various hardware and software requirements. Some of the requirements were determined at the beginning while others were derived during the process of research.

1. In order to construct a 3D model of the wind turbine blade, several different views, i.e. 2D images of the blade are required. These images combined must span the entire length, breadth and height of the blade.
2. A suitable pattern must be determined for the drone such that the images captured by the camera mounted on the drone must satisfy the criteria specified in the earlier requirement.

3. The system must account for sudden gusts of wind and wake effects which may cause unpredicted displacement of the drone from its expected position.
4. The proof-of-concept system must be constructed using commercial, easily-available technology in order to demonstrate the economical feasibility and ease of implementation of the suggested approach.
5. The hardware constraints of the unmanned aerial vehicle such as speed, size, battery and flight time must be considered and its suitability for use in the proposed system must be evaluated beforehand.
6. The 3D model generated should possess sufficient detail such that strain or deformation in the blade is accurately detected and localized.
7. The 3D model should be generated from the set of 2D images in real-time.
8. As the system encompasses a range of technologies, it must be possible to integrate these technologies to obtain an end-to-end flow with minimal amount of human intervention.

## 3.2 System Architecture

Keeping in mind the aforementioned requirements, a suitable system architecture is proposed. The system mainly consists of two modules which are further divided into components. The simplified architecture of the system is represented in Fig 3.1 The first module encompasses a learning algorithm which is responsible for the following functions:

- Determine a suitable path around the turbine blade using a mathematical model.
- Use a tracking algorithm to obtain expected positions of the drone at different times.
- Determine correction equations to account for wind gusts and unexpected drone movement.

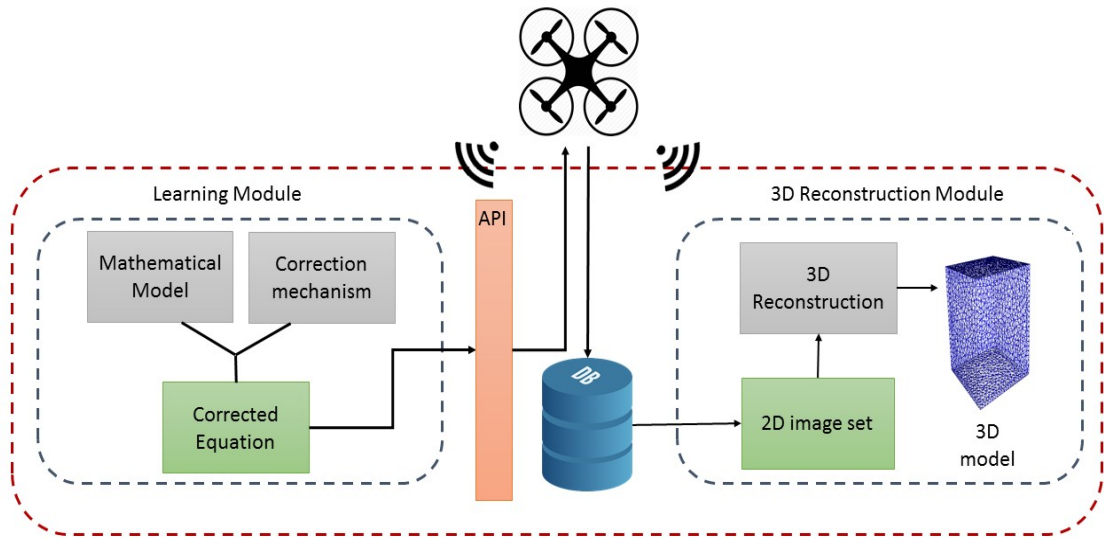


Figure 3.1: Simplified System Architecture

- Fly the drone using corrected equation around the turbine blade and capture images from vantage points.

The second module of the system uses computer vision and image processing concepts to construct a 3D model from the 2D images obtained. The functions of this module are listed below:

- For each image, identify feature keypoints that can be matched in other images.
- Compare the identified keypoints with keypoints in every other image and perform 3D stitching when a match occurs.

### 3.3 Learning Module

The Learning Module computes the path of the drone using a mathematical model so that it can be flown autonomously around the blade. A tracking algorithm is used to establish corrections in positions of the drone due to the effect of winds and other natural

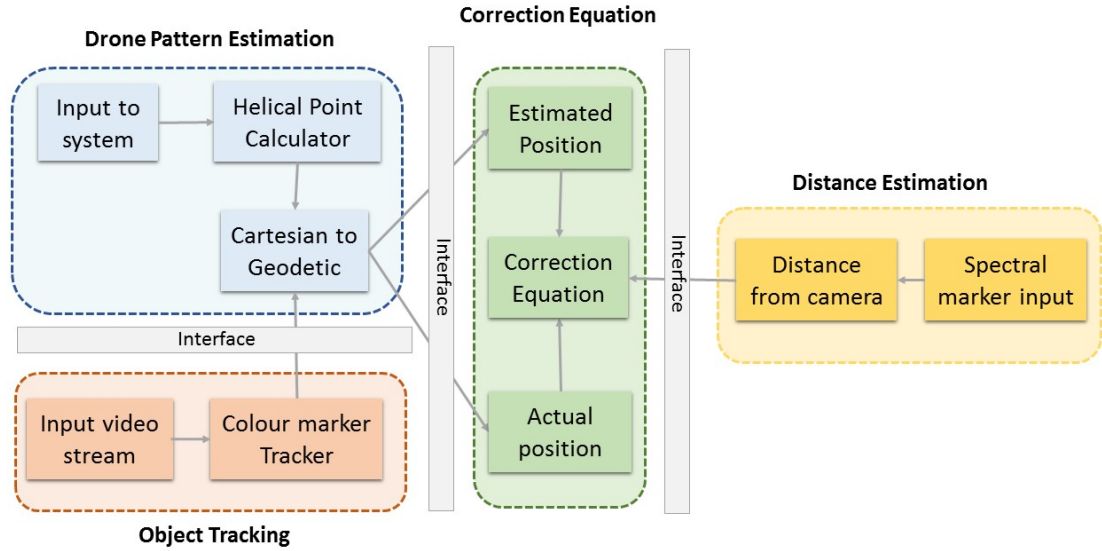


Figure 3.2: Architecture of the Learning Module

factors. The Learning module is comprised of various components which are represented in the Fig 3.2. Each component of the system is described in the following subsections.

### 3.3.1 Drone pattern Estimation

A helix is chosen as a suitable model for the path of the drone around the wind turbine blade. A helical path is an ideal choice in this case as it not only covers a circular arc around the blade to obtain images from various angles but also provides a stepwise linear increment in height. By choosing various vantage points around the drone on a helical curve, it can be ensured that the images captured will cover all surfaces of the blade.

#### Helical Pattern

A mathematical model can be used to rotate the drone in a helical fashion around a stationary blade. There are three kinds of helical structures namely Circular Helix, Cylindrical Helix and Slant helix. For the stationary wind turbine blade, a cylindrical helix model is chosen. The required helix is first constructed in the Cartesian coordinate system and

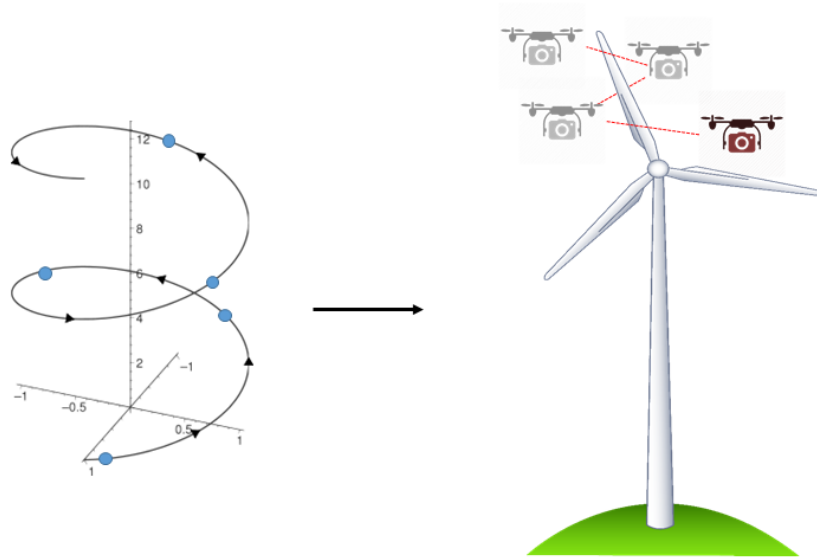


Figure 3.3: Identifying points on helix and conversion to real-world coordinates

then translated to real world coordinates as shown in Fig. 3.3. The parametric equation of a helix in the Cartesian system is given by:

$$x = r \cos \theta$$

$$y = r \sin \theta$$

$$z = b \theta$$

for  $\theta \in [0, 2\pi]$  and  $b$  is a constant given by  $\frac{h}{2\pi}$  where  $h$  is the height of the helix and  $r$  is the radius of the helix .

### **Translation of helical pattern to real world coordinates**

From the above parametric equation, we can obtain points on a helix by varying the value of  $\theta$  in constant increments. These points need to be converted from the Cartesian system into real world co-ordinates. To achieve this, the  $(x, y, z)$  coordinates of the helix are converted to Global Positioning System coordinates in decimal degree format, i.e., to corresponding Latitude, Longitude and Elevation values.

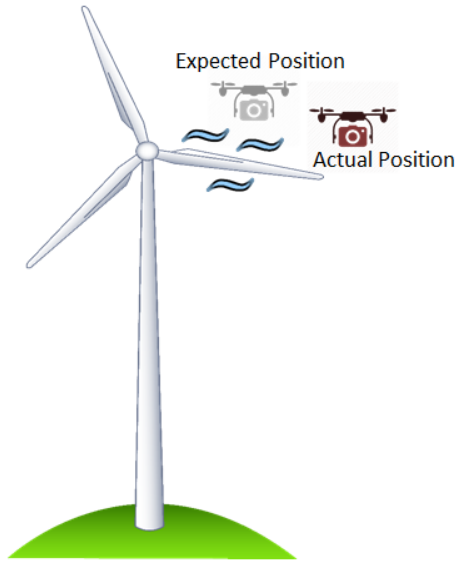


Figure 3.4: Difference between estimated and actual position due to wind and wake effects

### 3.3.2 Object Tracking

Although the above approach seems to provide a robust solution, the presence of wind and aerodynamic noise may cause the drone to move to a different position instead of the expected position. Commercial drones have mechanisms to remain stationary in the presence of winds by increasing the speed of the propeller blades in the direction opposite to wind, however this is not very effective while the drone is in motion. Since the size of modern quadcopters is quite small, it may be blown some distance away by a strong gust of wind. This is represented in Fig 3.4.

In order to estimate the difference between the expected position and actual position of the quadcopter, we compute positions of the drone by identifying spectral markers in images captured by the drone at various points. The quadcopter can be made to detect and track a colored marker on the surface of the blade by segmenting the markers in the incoming input image stream. Using this method, the actual position of the drone at a particular point can be calculated.

This approach however has a few limitations. The tracking of the coloured marker is done in the 2D system, however the required co-ordinates of the point should contain three dimensions. The  $x$  and  $y$  coordinates can be estimated from the position of the marker in the captured image, however the  $z$  coordinate which represents the distance from the blade cannot directly be obtained through this method. A simple alternative has been suggested to rectify this.

### 3.3.3 Distance Estimation

The distance of the camera from the turbine blade can be calculated using a simplistic approach of detecting two different spectral markers on the blade in an image frame instead of a single colored marker. If the focal length of the camera is known, this reduces to the problem to one of triangulation. The distance of the camera  $D$  from the blade can be derived by using the formula

$$D = \frac{W * F}{P}$$

where  $W$  is the distance between the two markers on the blade,  $F$  is the focal length of the camera and  $P$  is the pixel distance between the two markers in the captured image. This can be further simplified by using two differently coloured markers which can be tracked easily by the drone. This has been shown in Fig 3.5

### 3.3.4 Correction Equation

By making use of the methods mentioned above, the expected and actual positions of the drone are computed. The error is calculated as the linear displacement in the three directions  $x, y$  and  $z$ , and is given by

$$\delta x = x_{exp} - x_{act}$$

$$\delta y = y_{exp} - y_{act}$$

$$\delta z = z_{exp} - z_{act}$$





Figure 3.5: Tracking two differently coloured spectral markers

where  $(x_{exp}, y_{exp}, z_{exp})$  are the coordinates of expected position of drone and  $(z_{act}, z_{act}, z_{act})$  are the coordinates of actual position of drone. This method linearizes the points observed on the helix and simplifies the error calculation to simple linear translation rather than a differential equation.

To improve accuracy of this approach, a machine learning algorithm can be implemented to learn the error ranges and calculate an approximate error model for various wind speeds in a particular area. During the training phase, the actual and expected positions are computed during different times when wind speeds may be different. Based on the range of errors obtained, a mean value of error is computed which will be used for correction during the testing phase. The corrected equation is given as

$$\begin{aligned}
 x_{final} &= r \cos \theta - \delta x \\
 y_{final} &= r \sin \theta - \delta y \\
 z_{final} &= b \theta - \delta z
 \end{aligned}$$

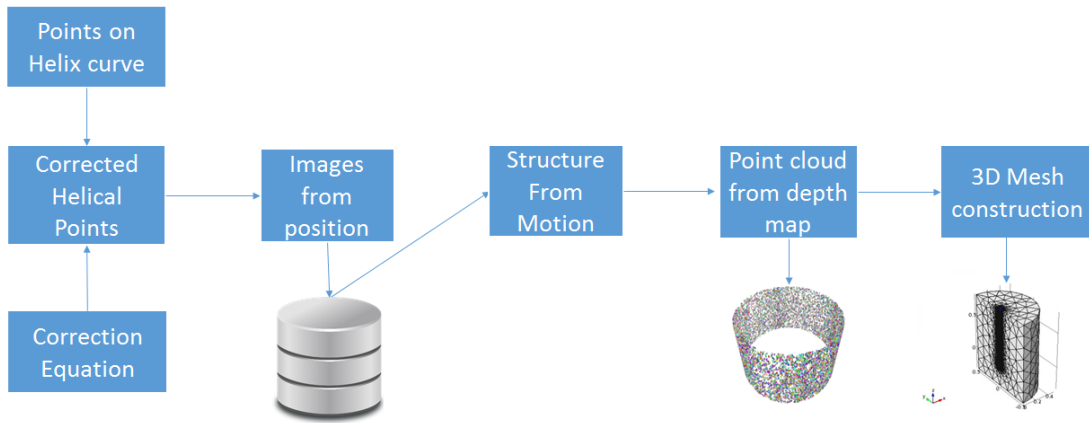


Figure 3.6: Steps in 3D Reconstruction Module

At each corrected point  $(x_{final}, y_{final}, z_{final})$ , a two dimensional image of the blade is captured at a fixed distance from the blade.

### 3.4 3D Reconstruction Module

This module retrieves the image set captured by the quadcopter at various points and processes it into a three dimensional model in real time. By incorporating a high level of detail into the 3D model, deformities, delamination and cracks can be detected and localized in the wind turbine blade. The ‘Structure-from-Motion’ framework which uses SIFT Feature Detection multi-view stereo vision is used to compute the 3D model of the turbine blade. The steps in conversion of the 2D images set to the 3D model is diagrammatically represented in Fig 3.6.

#### 3.4.1 Structure from Motion

The ‘Structure from Motion’ framework is used to convert 2D filtered images to a 3D Point Cloud or Mesh Model. The 3D model is then examined for cracks, bends or other deformation by a human operator. The Structure from Motion Pipeline is described in a series of steps listed below:

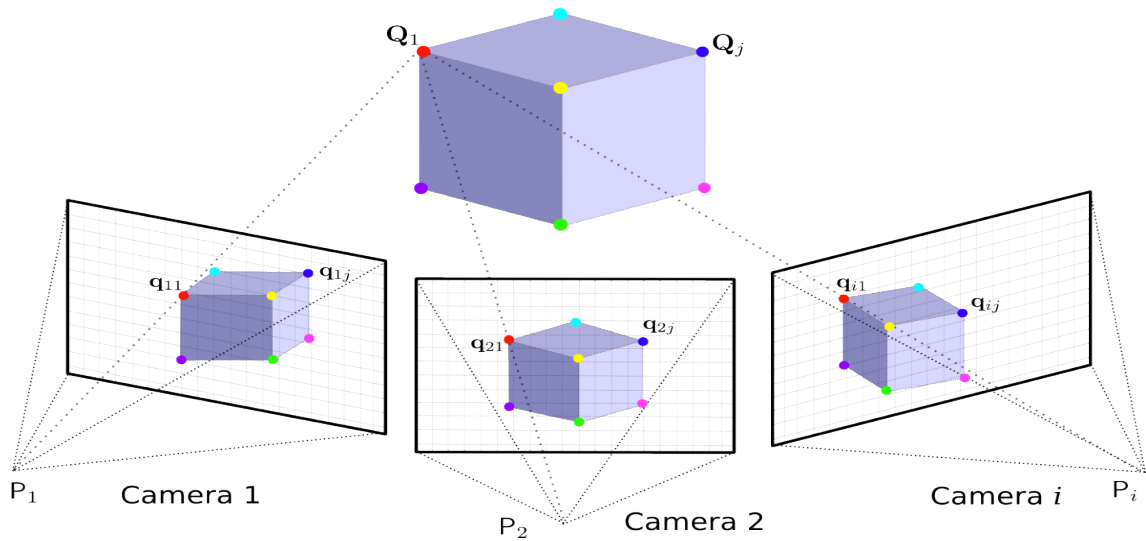


Figure 3.7: Object Estimation from Structure from Motion [Snavely2008]

- Create a 2D image set such that each image provides a different view of the object or scene whose 3D model needs to be constructed.
- Identify SIFT features in each image that can be detected and matched in other images.
- Search for corresponding feature matches in other images.
- Compute camera positions and point positions in the image such that the viewing rays intersect.
- Filter out false matches by applying visibility constraints.
- Apply a Bundle Adjustment algorithm for corrections and smoothing surfaces.
- Compute surface from 3D points by developing a mesh model or point cloud.

### 3.5 Design Challenges

To effectively monitor a stationary wind turbine blade using an unmanned air vehicle, certain key design aspects needed to be considered. Some important design challenges along with corresponding decisions are listed below.

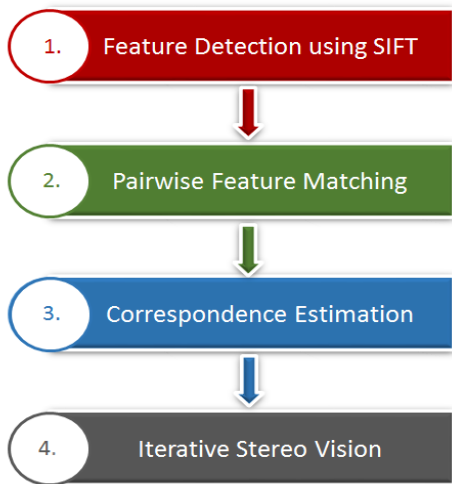


Figure 3.8: SFM Workflow

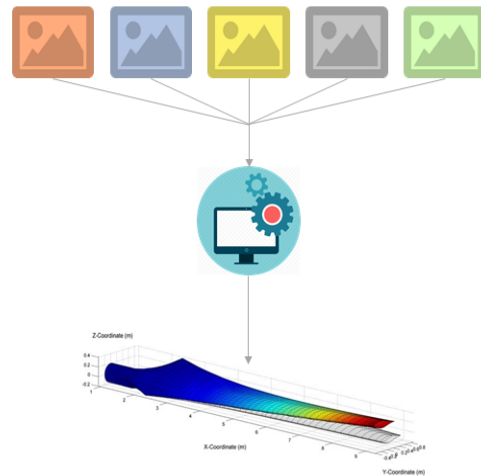


Figure 3.9: 3D Reconstruction using SFM

1. *A simple yet effective pattern for the quadcopter's motion around the blade should be determined.*

A helical or spiral pattern would be ideal in this case as it provides a  $360^\circ$  view around the surface of the blade. The step wise increment in height at each point makes it even more beneficial as a gradual increase in height and can provide views that differ slightly in angle which allow for greater overlap and more feature matches between images. This pattern is also sufficiently complex, and can be used to effectively utilize the autonomous, unobtrusive monitoring and flight capabilities of the drone.

2. *It must be possible to achieve an end-to-end flow in the system by interfacing separate components of the system*

The various components of the system may be developed using different technologies and integration of these components will pose an interesting challenge. As this project is divided amongst various separate fields of research such as robotics, civil engineering, computer vision and machine learning, languages and libraries that can be easily integrated are chosen and combined together to achieve an end-to-end flow. The 3D reconstruction module and the Learning algorithm will not need to

be integrated as the drone flight logically separates these two components of the system.

3. *A suitable 3D reconstruction mechanism must be chosen to construct the 3D model*

As the speed of the drone is quite high, its movement in a helical pattern will generate a stream of images at rates similar to those in video capture. For this reason, the ‘Structure from Motion’ framework which produces accurate 3D models and meshes from a video stream or a continuous sequence of input images is determined to be suitable.

## 3.6 Summary

This chapter presented an overview of the requirements of the proposed system derived from the research objective. The system architecture is specified which consist of 2 parts - the Learning Module and the 3D Reconstruction Module. The Learning Module determines the pattern that the quadcopter must follow, points on the path at which images must be captured and corrections in the presence of wind and wake effects. A helix is chosen as the most suitable model. The 3D Reconstruction Module provides a framework through which a set of 2D images that furnishes different views of a scene or object can be used to construct a 3D point cloud or a three dimensional mesh model. The Structure from Motion algorithm using SIFT keypoints is used to achieve this. Finally, some of the design challenges that were faced during the course of the research have been presented along with resulting design decisions.

# Chapter 4

## Implementation

This chapter discusses the methods and technologies which can be used to develop a system based on the design concepts discussed in Chapter 3. First, each component in the system is described in detail along with the algorithms, methodology, language and libraries that have been used for its implementation. Next, the integration of the various components of the software and hardware are described. Finally, the end-to-end flow of the system is described along with a short summary.

### 4.1 Helical Path of the drone

#### 4.1.1 Cartesian construction of helix

Using the parametric equation of the helix, an arbitrary number of equidistant points are chosen on each spiral of the helix. Linearization of the helical pattern using a fixed number of points greatly reduces the complexity of the problem. For a larger wind turbine blade, the number of points chosen will be high while a smaller blade may require fewer points because of greater overlap of views from individual points. Large numbers of images greatly increase the complexity and load on the system so the number of points must be optimized such that a minimum number of images are captured in order to produce a sufficiently detailed model for the turbine blade in consideration. Each of the points

```

Begin
NumofHelixSpirals= (Blade Length/VerticalHeight);
θ = 0;
height = h; // spiral height h
For i: 1 ->NumOfHelixSpirals
    For j: 1->NumOfPointsOnSpiral(n)
        θ = θ +  $\frac{2\pi}{n}$ 
        Calculate (x,y,z) from the equation of helix
        //Points on each spiral arc obtained
    End for
    height = height + h;
End for
    //iterate over different spirals
End

```

Figure 4.1: Algorithm for generating points on Helix

on a single spiral arc is obtained by varying the value of  $\theta$ . ‘ $n$ ’ equidistant points on a single spiral of the helix are chosen by splitting the angle of a circle into  $n$  equal parts. Hence each point  $(x_i, y_i, z_i)$  on the spiral is obtained by varying the angle  $\theta$  in stepwise increments of  $\frac{2\pi}{n}$  such that  $\theta = \frac{2\pi}{n}, \frac{4\pi}{n} \dots 2\pi$ , where  $i = 1 \dots n$ . The points on subsequent spirals in the helix are obtained by varying the height ‘ $h$ ’ of the helical arc for the spiral in consideration.

The diameter ‘ $d$ ’ of the helix is given by

$$d = \text{Longest Cross Section of Blade} + (2 * \text{Distance of camera from blade})$$

The drone is positioned at a minimum distance of 8 metres in the blade. This is to account for the wind turbine blade’s vibrations which may cause collision between the drone and blade and also to ensure sufficient level of detail in captured images. The vertical area captured by the camera can be calculated using the focal length of the camera lens. The HD camera mounted on the DJI Phantom Vision Plus has a focal length of 5mm and can capture a vertical height of 7.63 meters of the object while flying at distance of 8 meters from it. This maximum vertical height forms the height ‘ $h$ ’ of the helix. The pseudocode

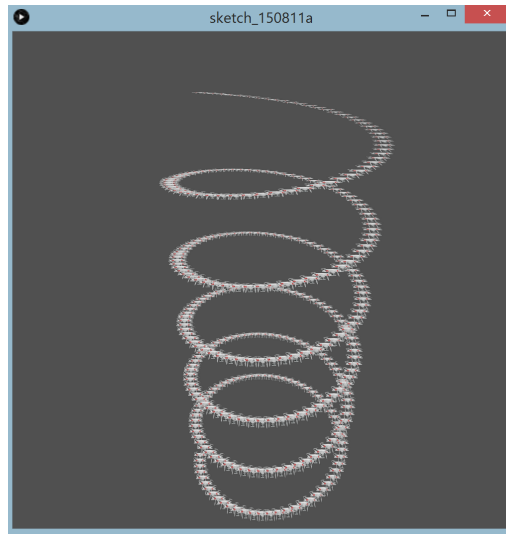


Figure 4.2: Processing Sketch to validate helix algorithm

to obtain points on the helix is presented in the Fig 4.1.

The above algorithm is implemented in Java and points are generated on the helix based on the blade length entered and the radius of the helix calculated. The points obtained are plotted on a console to test the accuracy of the algorithm. This is done using a ‘Processing’ sketch as in Fig 4.2. Once the algorithm is validated, required points on the helix are computed based on the blade length and radius.

### 4.1.2 Cartesian to Geographic Co-ordinates

From the earlier step, the Cartesian coordinates of various points on the helix pattern can be computed. In order to facilitate revolution of the drone about an actual wind-turbine blade, the points should be mapped to real world coordinates. This can be done in one of two ways:

- Conversion of Cartesian Coordinates to GPS and Elevation
- Conversion of Cartesian Coordinates to Euler Angles (Roll, Yaw & Pitch).



The proposed system will make use of the first method of conversion to GPS as it allows easy integration of model with the drone. To achieve this conversion, the system datum (World Geodetic System 84) is used. Other methods of converting Cartesian coordinates to cartographic coordinates include Bowring's algorithm(1985) and the Heiskanen algorithm. The WGS 84 standard assumes the center of mass of earth as a reference point and an ellipsoid reference shape. The WGS 84 conversion has been implemented in Java by using the 'AGI.Foundation.\*' libraries and integrated with the system elements described in Section 4.1.1.

The combined code takes the length and maximum cross-section of the turbine blade as input and computes the Cartesian and Cartographic coordinates of points on a helix curve around the blade. The origin is assumed as the hub of the wind turbine so that the necessary elevation for the points can be calculated. The hub is assumed to be at a height of 150m from the ground for experimental purposes. This allows each point obtained in the previous step to be converted to Latitude, Longitude and Elevation values in the decimal degree format.

### **4.1.3 DJI GroundStation Waypoints API**

The Latitude, Longitude and Elevation values computed are directly interfaced with the drone's API in order to achieve autonomous flight. The path of the drone from one point on the helix to other takes place in a linear fashion and does not follow an arc. To achieve a circular arc between points, Euler Angles must be used. The geodetic coordinates obtained are fed into the DJI Phantom 2 Vision Plus drone using the DJI GroundStation Waypoints API which flies the drones autonomously between the specified locations.

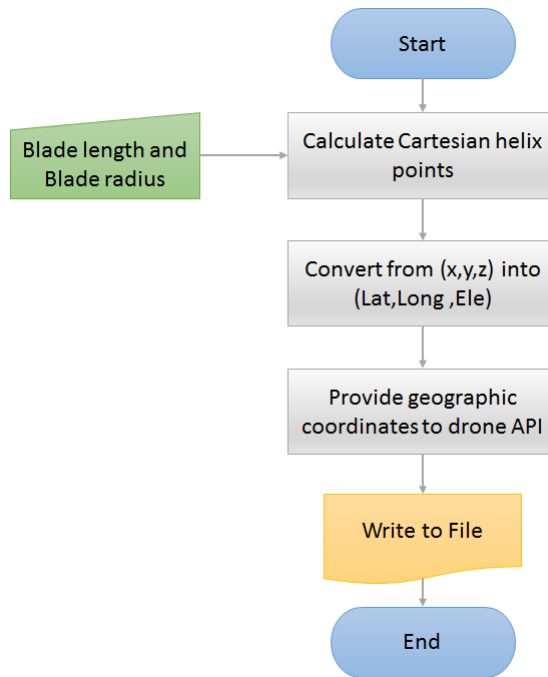


Figure 4.3: Calculation of Helical Points around blade

#### 4.1.4 Summary

This module produces a linearized Helical path of the DJI Phantom drone along the wind turbine blade. By using the blade length and blade radius as input, the parametric equation of the helix is used to compute various points on the helix. These points are converted from Cartesian to Geodetic coordinates which are then fed into the DJI Phantom 2 Vision Plus drone via the DJI Ground Station Waypoints API to obtain an automated helical path around the blade. The workflow of this component is represented in Fig 4.3

## 4.2 Marker Tracking using Quadcopter

The GPS locations determined in the earlier step may contain some inherent error in positional accuracy, which typically ranges to a few meters of length. For this reason, a mechanism that is independent of GPS needs to be chosen in order to estimate the error between expected and actual positions. This divided this into a series of steps:

1. Track colored marker in video stream and determine its coordinates
2. Identify atleast two differently colored spectral markers in the image and calculate distance between them in order to calculate the distance of camera from the blade.
3. Track motion in the absence of colored markers.

#### **4.2.1 Tracking motion using a colored marker**

By placing a colored marker on a moving object, the motion of the object can be tracked easily. The image can be thresholded in order to separate the colored marker from the rest of the image. The coordinates of the centroid of the bounding box that contains the segmented marker region can provide a reference point for the position of the object in the video frame or image sequence.

First, the input image or video is converted from the RGB color space to the HSV color space as colored objects can be tracked more easily and accurately using Hue, Saturation and Value components. The HSV ranges for a particular color are determined either through trial and error or more efficiently using a machine learning algorithm as shown in Fig 4.4.

Next, objects of a particular color in the image are segmented by thresholding using the range of hue, saturation and value determined in the previous step. All the pixels whose values lie between the maximum and minimum values in the range are extracted from the image. Erosion and Dilation are performed after thresholding in order to eliminate noise.

In the final step, contours are identified in the binary threshold image obtained. Using the ‘moments’ method, the longest contour in the frame is determined and the (x,y) coordinates of each of the points on the longest contour are retrieved. The centroid of the largest white region in the binary image is obtained by averaging all points on the

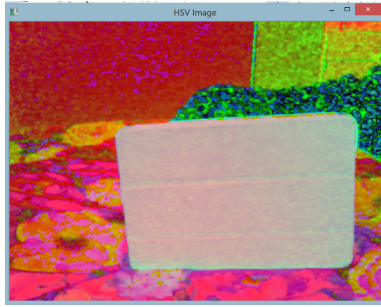


Figure 4.4: HSV Image

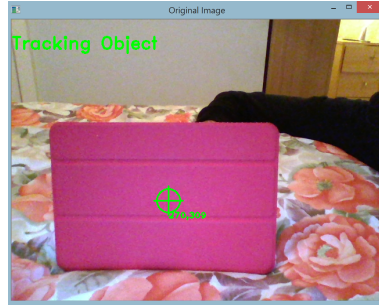


Figure 4.5: Color Tracking

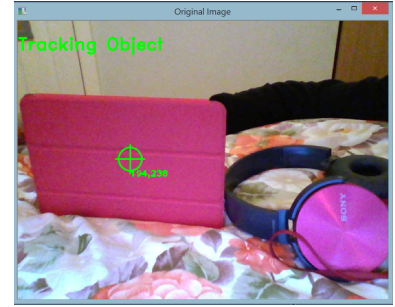


Figure 4.6: Longest contour

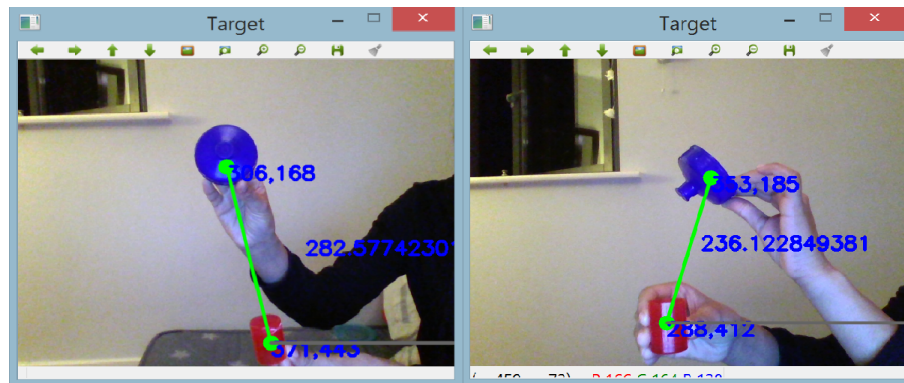


Figure 4.7: Pixel distance between two colored markers

contour. These steps are shown in Fig. 4.5. This algorithm is implemented using C++ and OpenCV 2.4.10.

#### 4.2.2 Tracking differently colored moving objects

By tracking two spectral markers in a frame instead of one, the pixel distance between the markers in the image captured can be used to gauge the distance of the drone from the blade as an alternative to using ranging mechanisms such as acoustic or ultrasonic reflection. The pixel distance between the markers can be obtained by calculating the Euclidean distance between the bounding box centroids of the two markers in the Fig 4.7. In the simplest method, the distance of blade from the camera can be obtained by using the focal length of the camera, the pixel distance between the markers and the actual distance between the markers using the formula

$$DistanceFromCamera = \frac{FocalLength * ActualDistanceBetweenMarkers}{PixelDistanceBetweenMarkers}$$

By applying this formula to the incoming video stream or image sequence, the distance of the drone from the blade can be calculated. The pixel distance calculated in the earlier step is applied along with the focal length of the camera (5mm for a DJI Phantom Vision Plus quadcopter with a mounted HD 1080p camera). An arbitrary distance of 5meters is considered as the actual distance between the spectral markers. In a system where distances are continuously calculated for each incoming frame an additional control can be setup which ensures that the drone stays within a range of distances from the blade. This has been implemented using Python(X,Y) and OpenCV 2.4.10.

### 4.2.3 Sequential Differencing to identify motion

This method is used to track a moving object in the input video stream or in a sequence of images. Two sequential images from an input stream or from a video are read by the system. The pixels in the two images are compared in order to detect what pixels have changed with between them. This can be obtained by computing difference between successive frames and using a difference image in order to identify the changed pixels. A threshold is applied to the difference image in order to clearly segment the moving object. Erosion and Dilation are performed on the threshold image to eliminate false positives and false negatives in the presence of noise. Finally a bounding box is drawn over the segmented area and the centroid is highlighted and labelled with its 2D coordinates to facilitate easy following and tracking as shown in Fig 4.8.

This approach is used to detect whether the blade is stationary or in motion without the need for colored markers, and to follow the blade's trajectory in 2D in the absence of spectral markers on the blade. This is implemented using C++ and OpenCV 2.4.10.

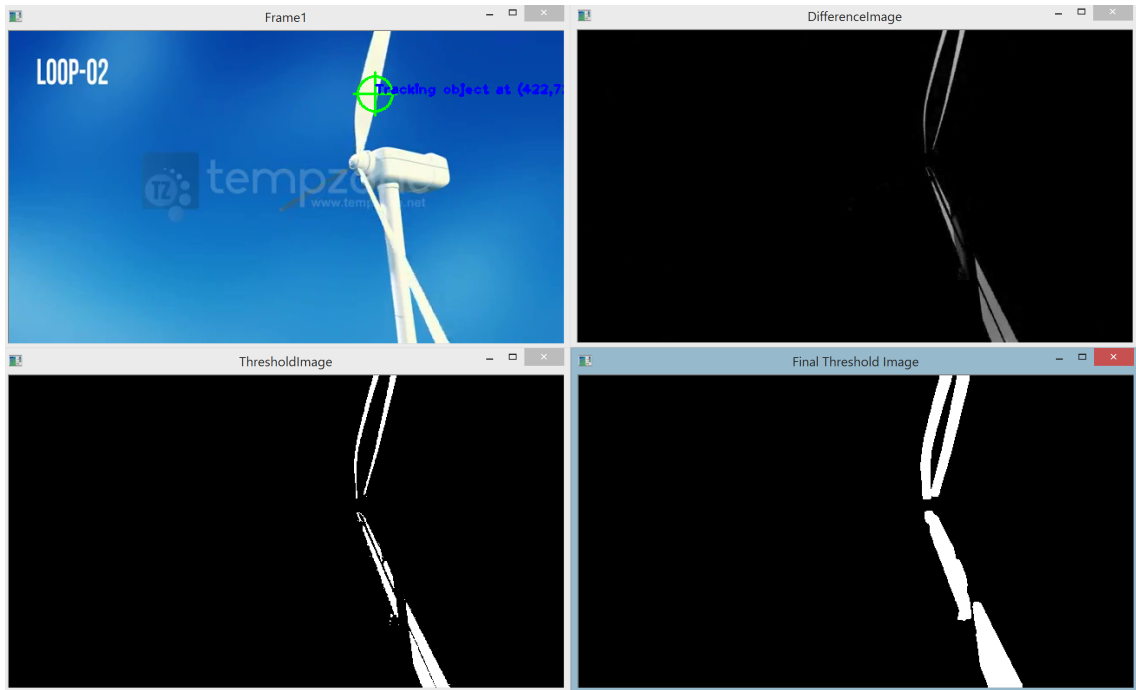


Figure 4.8: Object tracking without color

#### 4.2.4 Summary

This module enables the drone to move in a specific pattern around the wind turbine blade without the need for GPS locations to be supplied beforehand. The drone can be programmed to follow a colored marker at a specified distance from the blade. Distance between the blade and drone can be evaluated from the image sequence by calculating distance between differently colored markers in the image and comparing the pixel distance to the actual distance between the two markers. In the absence of spectral markers, collision between the blade and the drone can be prevented by detecting object motion without spectral markers through the method of sequential frame differencing.

### 4.3 3D Reconstruction from 2D Image Set

Once the drone's pattern is established, images are captured from different vantage points on the helix which are used to construct a 3D model of the blade in real time. For this purpose the 'Structure-from-Motion' approach is used. Our end product is a 3D point

cloud or mesh model with sufficient detail to detect and localize deformation or damage in the blade.

### **4.3.1 VisualSFM**

A popular Structure-From-Motion framework 'VisualSFM' is used to compute the 3D point cloud. This software, developed by Changchang Wu, makes use of SIFT using Gaussian pyramids and Multicore Bundle Adjustment along with multi-view Stereo Vision in order to compute a 3D point cloud of the object[Wu2011].

This application can be used for sparse 3D reconstruction based on the keypoints identified by the algorithm. It takes the 2D image set as input, checks each of the images for SIFT features and looks for these feature matches in all other images as shown in Fig 4.9. If feature matches are found, the corresponding views of the features are used to establish a depth map between points in the image. By performing this operation for each of the images in the image set, most of the matches are correctly obtained. One major drawback of this algorithm is that is not robust to illumination changes such as shadows and noise, and hence cannot be used to construct a very accurate 3D model. The output of this tool is a set of perspective images and calibration parameters of the camera based on the images that have been captured. A limitation of Visual SFM is that it cannot be used effectively for dense keypoint match computations. It can be integrated with the PMVS/CMVS tool developed by Yasutaka Furukawa to obtain a dense 3D perspective.

### **4.3.2 CMPMVS**

The sparse or dense 3D perspectives obtained from Visual SFM must be converted to a suitable form through which it can be viewed as a 3D model. Moreover, the model should have the ability to be viewed from different perspectives. CMPMVS, developed by Michal Jancosek and Tomas Pajdla [Jancosek201], is a 3D reconstruction software

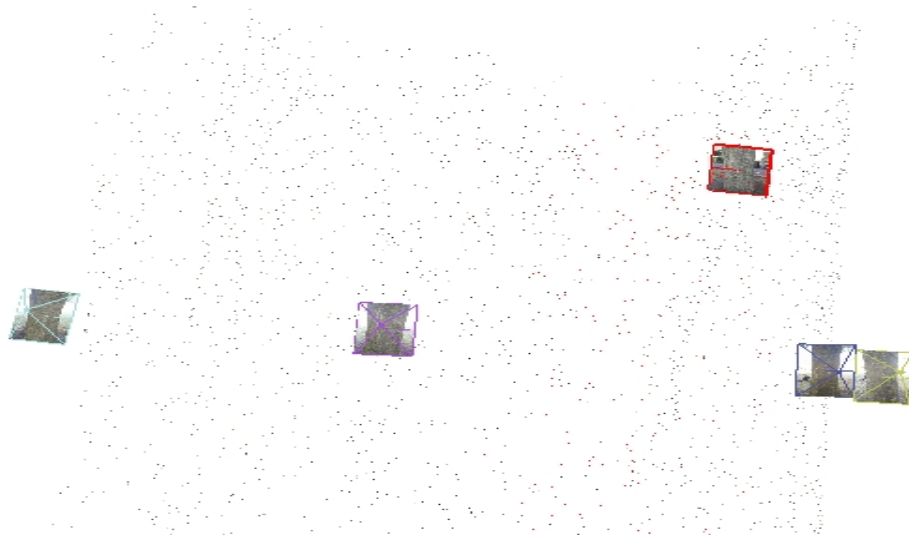


Figure 4.9: Computation of SIFT points and perspective images in VisualSFM

used to construct a mesh model from a set of perspective images. Based on the matched features, perspective images and intrinsic and external camera calibration parameters, a dense 3D point cloud is computed which consists of the object's feature keypoints from perspectives. In the absence of spectral markers, VisualSFM and CMPMVS provide a very, poor inaccurate model of the scene. Hence, for this approach to be used effectively, spectral markers need to be added to the surface of the blade.

### 4.3.3 MeshLab

Meshlab is an open-source, lightweight tool that can be used to view, edit and render structured and unstructured meshes. This software is used to correctly display and render the mesh model constructed by CMP-MVS in the previous step. The processing capacity of MeshLab is quite low and can only be used to view and render meshes that are less than 100Mb in size. This implies that specialist 3D rendering software will be required to produce blade models with high amounts of detail. A mesh created using CMP-MVS and rendered using MeshLab is shown in Fig. 4.10



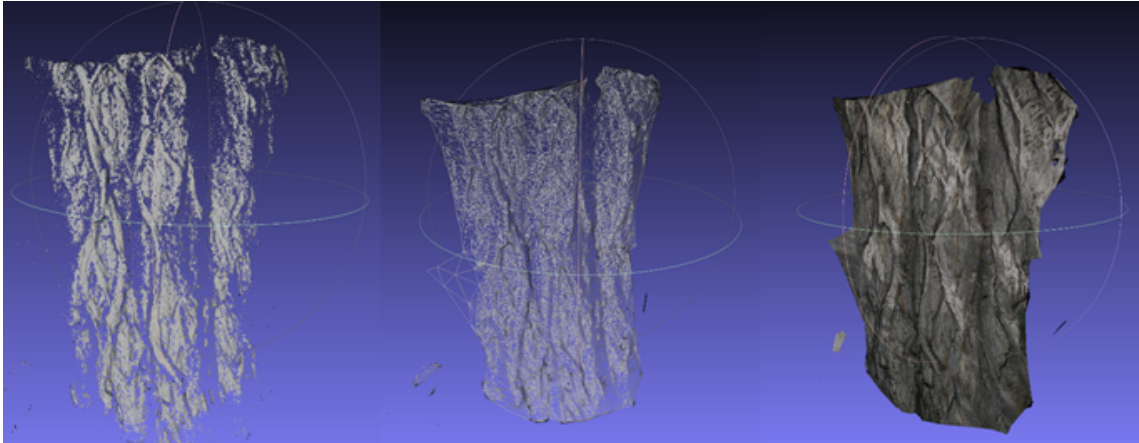


Figure 4.10: 3D point Cloud, Mesh and texture rendered using MeshLab

#### 4.3.4 Blender

Blender is an open-source image processing, computer graphics and animation software that can be used for creation, modeling, simulation, filtering and rendering of 3D graphical structures. Blender will be used to render and filter high-definition meshes that cannot be processed by MeshLab as shown in Fig 4.11.

#### 4.3.5 Summary

The 3D Reconstruction Pipeline is described in this section. VisualSFM is used to match SIFT Features, estimate camera calibration parameters and generate perspective images that provide an idea about the position of the camera while capturing the image. CMP-MVS takes the perspective images from Visual SFM and constructs a sparse or dense 3D mesh. The generated mesh can be viewed as a point cloud, a mesh structure or in its rendered form in MeshLab or Blender.

### 4.4 Integration

Various technologies are used to implement the above system. In order to integrate the different components of the system and obtain an end-to-end flow end-to-end workflow, certain simplifications have been used due to the time constraints of the project. The

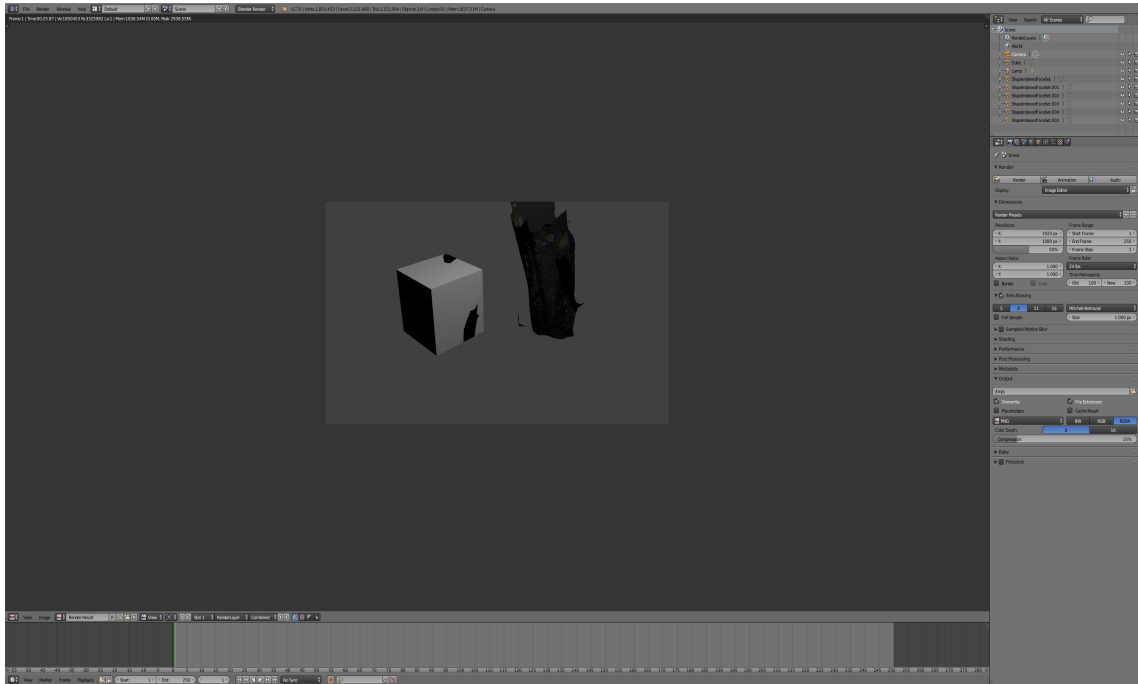


Figure 4.11: Dense 3D Mesh rendered using Blender

GPS co-ordinates of the Helix path from the Java implementation are written to a file from which it is read by the DJI Ground Station API to set waypoints for the drone. The different marker tracking algorithms that have been developed using OpenCV, Python and C++ are integrated into a single component by importing the Python library in C++ and embedding the Python snippets within the C++ code.

## 4.5 Implementation Challenges

Numerous challenges were faced during the implementation of the system. Some of them are listed below:

1. Conversion of  $(x,y,z)$  to GPS  $(Lat,Long,Ele)$  is challenging.(WGS 84)
2. Very short distance errors cannot be reliably obtained by GPS.
3. Image processing software requires high computational power
4. Object tracking in 3D is complex.

5. Two-camera stereo vision depth maps are not very accurate as point cloud is generated using only 2 images.
6. Large meshes are not very easily rendered, and cannot be processed efficiently using open source tools.
7. Spectral or SIFT patterns must be present on the surface of the blade for the chosen approach to work.

## 4.6 Overall Summary

Different technologies and software were evaluated for suitability for developing the system according to the design specifications. Initial experiments attempted to create the helical pattern of drone by providing values of drone parameters (roll, yaw, pitch and uplift) for path between two consecutive points on helix. This proved to be highly complex and did not provide good results during simulation through the Heli - X Quadcopter Simulator. The linearization of the steps in the helix and conversion to GPS greatly simplified the problem and allowed effective vantage points to be determined on the surface of the helix. Wake and wind effects have been accounted for by implementation of the marker and motion tracking algorithms which are used to determine the position errors obtained during different wind speeds. 3D reconstruction was initially attempted using stereo vision however the results weren't accurate enough to detect deformities or cracks in the blade. After extensive research, the SFM framework was determined to be suitable for achieving the objective of the system. All parts of the system have been successfully implemented but the integration requires refinement. Most of the testing of the system has been done using software simulators. The next step would be to test the system on a wind turbine blade in outdoor settings.

# Chapter 5

## Evaluation

This chapter presents an evaluation of the proposed system which gives an indication of the system performance. As this system contains various disparate modules, different experiments are conducted to measure the efficacy of each of these modules individually and for the system as a whole. The aim of the experiments conducted is to obtain an overall understanding of the efficiency, reliability and usability of the proposed system.

### 5.1 Rationale

Before the experiments are discussed in detail, it is important to understand the factors that affect the proposed system and metrics that can be used to measure the performance of the system.

#### 5.1.1 Factors

The proposed system is composed of several different components which are responsible for various functions of the system. Factors which affect different aspects of the system are considered and these will also play an important role in the overall efficiency of the system.

1. **Distance of the drone from the blade:** The distance of the drone from the

blade is important to determine the range of distances between which the flight of the drone must be restricted in order to obtain suitable results and maintain acceptable safety margins. The minimum distance of the drone along its linear path from one point on the helix to another also plays an important role as sufficient distance should be maintained to avoid collisions with the blade.

2. **Presence of noise during image capture:** The presence of noise or blurriness in the image being captured from camera may prevent the drone from following the marker correctly.
3. **Resolution and number of images captured:** The resolution and number of the images provided as input for 3D reconstruction will greatly affect the quality of the output 3D model. The time taken to process the images will also vary significantly based on these factors.

### 5.1.2 Metrics

Several metrics have been identified which can be used to evaluate the performance of the proposed system.

1. **Accuracy of Helix path:** The accuracy of the helical path of drone will determine whether the drone can actually move around the blade in a fashion that provides clear views from any vantage point while maintaining a minimum distance in order to avoid collision.
2. **Accuracy of marker detection and tracking:** The distance maintained by the drone from the blade and the presence of noise while capturing images such as blurriness due to rain, sudden wind etc. will determine how well the drone can detect and track the colored markers on the blade.
3. **3D Reconstruction time:** The time taken by the system to reconstruct the 3D model will a direct indicator of memory usage and system performance.

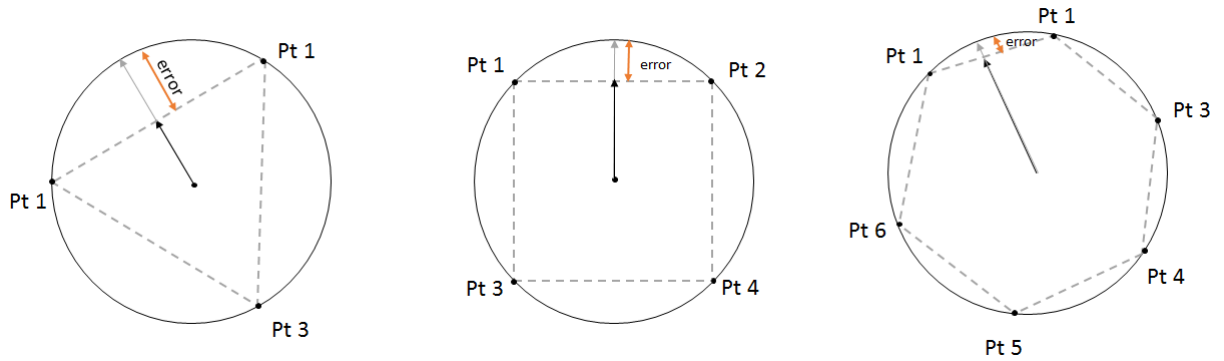


Figure 5.1: Distance error in linearization of helix(Top View)

4. **Quality of 3D model** :The quality of the 3D model will be the most important metric to determine the performance and reliability of the system as it must be detailed enough in order to accurately detect and localize cracks, structural deformities and damage in blade.

## 5.2 Experiments

The evaluation is conducted through three experiments which are described in detail in the following sections. The aim of the first experiment is to measure the disparity in distance of drone from the blade due to simplification of the helical pattern into a sequence of linearisations.

### 5.2.1 Experiment 1:

We consider a helix of radius 8 meters radius that is centred at the origin. We then estimate the distance between the path of the drone along the spiral arc and compare it with the closest distance between the line joining two points on the helix. This is represented in Fig 5.1. The minimum number of points per spiral is considered to be 3 as atleast 3 perspectives will be required to construct a three dimensional model. The height of the helix is assumed to be 12 meters. The percentage error in distance for different number of points on helix is listed in Table 5.1.

| Number of Points | Nearest Distance from blade(in m) |
|------------------|-----------------------------------|
| 3                | 4.46                              |
| 4                | 5.852                             |
| 6                | 6.997                             |

Table 5.1: Shortest Distance between drone and blade after linearization

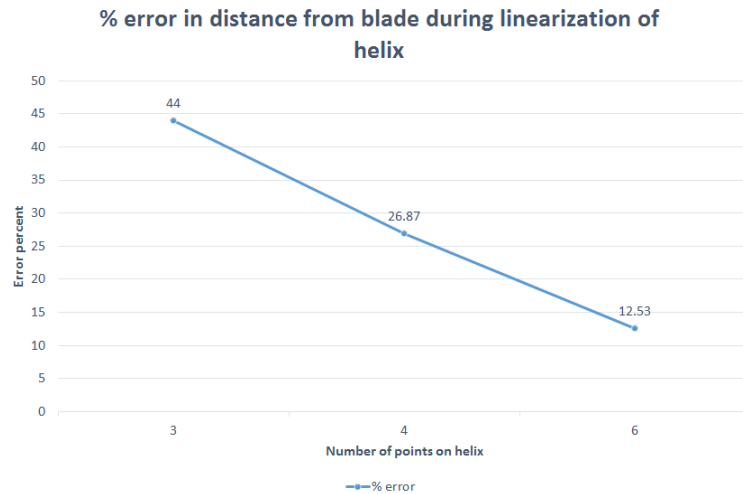


Figure 5.2: Percentage error in distance of drone from blade due to linearization of helix

The percentage error is calculated by measuring the perpendicular distance from the center of the helix to the line joining two consecutive points on the helix, and comparing it with the actual distance that it needs to maintain from the blade, i.e. 8m. From the observation it is evident that the greater the number of points on the helix, the smaller the error in distance. This is consistent with intuitive expectations. It can be concluded that in order to maintain a minimum distance of 8 meters between the drone and the blade, the error in linearization must be accounted for and the helix radius correspondingly corrected.

### 5.2.2 Experiment 2:

In the case of a sudden tilt or jerk of the drone, or in the presence of rain or other natural factors, the image captured by the drone may be blurred. This may also occur due to



Figure 5.3: Original Markers without blur



Figure 5.4: Markers with 13 % blur



Figure 5.5: Markers with 40 % blur



Figure 5.6: Markers with 60 % blur

overexposure of camera lens, incorrect focus and poor lighting levels. In such cases, the coloured spectral marker might not be detected accurately or may not be detected at all. This provides an indication that the image obtained by the drone cannot be used for 3D reconstruction as blurred features cannot be detected by the SIFT Feature Detection component of the ‘Structure from Motion’ approach. We have introduced a Gaussian Blur in the sample image to detect levels of blurring at which accurate detection of marker fails

By applying different sample horizontal and vertical blur levels to the sample image, levels upto which blurring can be handled by algorithm are detected. The graph shown in Fig 5.7 indicates the percentages of blur at which markers cannot be detected accurately. From experimental results, it is seen that the algorithm is robust up to 18% vertical and horizontal blur and produces moderate results for blurs ranging from 20-40%. These percentages can vary significantly based on the pixel area occupied by the marker in obtained image. In cases of higher blurring, the spectral markers are not detected as the algorithm



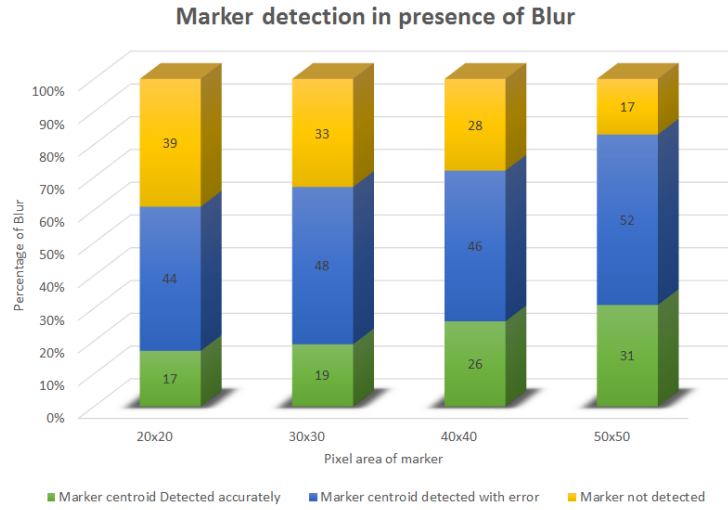


Figure 5.7: Marker Detection Accuracy vs Percentage of Blur

is unable to detect continuous contours. Marker images with different levels of blurring are shown in Fig 5.3, Fig 5.4, Fig 5.5 and Fig 5.6.

### 5.2.3 Experiment 3:

This experiment is used to determine the range of distances from the blade that the drone can maintain in order to acquire good quality images which can be used for 3D reconstruction. If the drone is too close to the blade, the spectral marker will appear large and the surface area of the blade being imaged will be correspondingly small. If the drone is overly far from the blade the features of the blade will be too small for effective integration in the 3D reconstruction.

In this algorithm, the minimum bounding box area for a marker to be detected is considered to be 40x40 pixels for an HD 1080 camera. If the area occupied by the spectral marker in the image is less than 40x40 pixels, it indicates that the camera is too far away from the surface of the blade to detect keypoints on the blade. For experimental purposes, two markers are assumed to be at a distance of 3 meters from each other on the surface of the blade. The farthest distance of the drone from blade is calculated using the principle

| Processing Times(in min) |           |           |           |
|--------------------------|-----------|-----------|-----------|
| Number of images         | 1920x1080 | 2048x1536 | 3120x4160 |
| 8                        | 35        | 54        | 65        |
| 15                       | 41        | 55        | 83        |
| 20                       | 60        | 65        | 86        |
| 25                       | 82        | 95        | 112       |

Table 5.2: Processing times for images of different resolutions

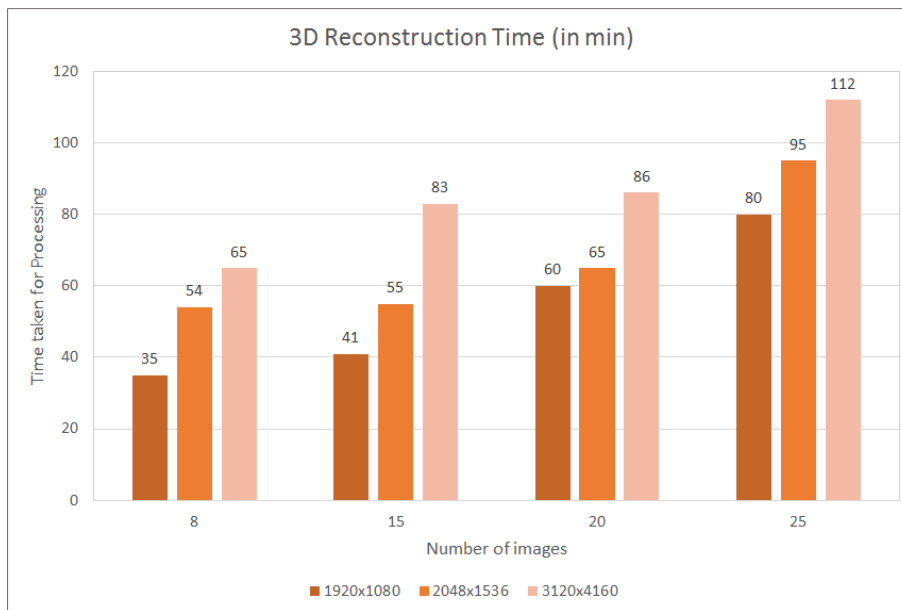


Figure 5.8: Time taken for 3D Reconstruction

of triangulation and estimated to be a maximum of 34.64 meters for the DJI Phantom Vision Plus camera. Similarly if the drone camera is too close to the surface of the blade, the keypoints will be magnified and blurred. Hence the drone must maintain a minimum distance from the blade. In order to account for vibrations of the blade in the wind and provide an appropriate safety margin, this distance is estimated at 8 meters.

#### 5.2.4 Experiment 4:

The time taken for the 3D reconstruction process greatly varies based on the resolution, size and number of input images. A number of models are created using different sets of 2D images at different resolutions. The time taken to process and render the final 3D

models is measured and compared to obtain an understanding of the memory usage and performance of system. All 3D model reconstructions have been performed on a system having 16GB DDR3 RAM and an UltraHD 3280 x 2160 display. The time taken for different image sets are represented in Table 5.2 and Fig 5.8.

### 5.3 Summary

Various metrics have been used to evaluate the performance of the proposed system. Based on the experiments and simulations conducted, the following insights have been gained:

- While moving the drone from one point on the helix to another, the motion is linearized and not an arc segment. This must be kept in mind while estimating minimum distance from blade.
- The system is robust to slight blurring, but does not currently provide sufficiently accurate results in the presence of high noise.
- The distance of the drone from the blade should lie within a threshold range which allows the features to be detected correctly
- The 3D model can be reconstructed in real time and the time taken is dependent on the number and quality of the images used.

# Chapter 6

## Conclusion

The first section of this chapter describes how the proposed system addresses the research questions set out at the beginning of the dissertation. The second section provides an analysis of the goals set and achieved during the course of the dissertation. The third section discusses future work to refine the system, and advance research from this point and the final section provides concluding remarks about the system.

### 6.1 Research Questions

This section addresses the research question posed at the outset of the research by addressing each of the sub-questions that arise from it. An overview of the approach used to tackle these questions are presented below:

*“Can visual imaging techniques be used to provide an efficient, unobtrusive and economical monitoring method for wind turbines?”*

The construction of a real-time accurate 3D model of the blade from its 2D image set using computer vision provides an efficient, economical, unobtrusive structural Health Monitoring technique. The 3D model developed can be analysed to identify cracks, strain, damage and deformation in the blade.

The subquestions arising from the research question are addressed below:

- *What kind of image processing algorithm can be used for structural health monitoring of civil structures?*

The construction of a 3D model of a civil or mechanical structure from various perspective images would provide an insight into the shape, texture and other physical attributes of the structure. Algorithms such as Stereo Vision, Feature Matching and Structure from Motion can be used to achieve this. Stereo Vision and Feature-based 3D stitching algorithms were implemented but did not provide satisfactory results. The 'Structure from Motion' framework demonstrated promising results and can be used for monitoring civil structures proactively.

- *How can the algorithm be extended to be robust if the target structure is in motion and not stationary?*

For moving structures such as Wind Turbine blades, the camera focus needs to be maintained on the surface of the blade so that different views of the blade can be obtained. This would be difficult to achieve using a stationary camera. By using a quadcopter mounted with a high definition camera, motion capability can be added to the camera and hence the camera can be effectively made to follow the wind turbine blade as it rotates. Hence, by leveraging the capabilities of an unmanned air vehicle with a camera, the algorithm specified earlier can be extended to moving structures.

- *What are other factors which come into play while monitoring a wind turbine in realistic outdoor environments?*

The locations at which wind turbines are installed are susceptible to a variety of natural factors such as wind, rain, sudden illumination changes etc. Wake effects also play an important role as they generate strong gusts of wind behind the rotating plane of the wind turbine. Due to all of these factors, the path of the drone may

change while in motion around the blade.

- *Can such a system be developed using commercial, easily available, off-the-shelf technology?*

The prototype of the system has been implemented using the DJI Phantom Vision Plus commercial drone and open source libraries from OpenCV, Python, VisualSFM and CPMVS. Although the model processed and rendered using these tools provides sufficient detail, specialist software will be required to produce accurate models with high levels of detail.

## 6.2 Conclusions

The proposed system was researched, designed, implemented, tested and evaluated during the course of the dissertation. Firstly, the helical path of the drone was achieved through simplification into linear steps. To account for displacement from the desired path due to natural factors like wind and rain, a correction equation is devised. Finally, a 3D model is constructed from 2D images taken from various points on the helix around an object. This has not been tested on a real blade but on a similar surface which contains optical markers for matching.

The contributions of this dissertation to the state-of-the-art are as follows:

1. Automation of quadcopter flight in a helical pattern:

Autonomous flight of quadcopters is an active area of research today as the use of drones increases. Estimating and automating different patterns of drone flight can be performed using a similar approach.

2. Color marker tracking by quadcopter on a moving wind turbine blade:

By tracking a colored marker on a moving turbine blade, a drone can be made to follow the circular path of a turbine blade in 2D and keep it in focus. This can not

only be used for health monitoring but also other surveillance applications such as following a moving vehicle.

3. 3D Reconstruction of Wind Turbine Blade The use of a 3D model for the purpose of Structural Health Monitoring is a novel approach and opens new potential areas of research.

### **6.3 Future Work**

There are a few limitations in the proposed system. The helical path algorithm can only be used to revolve the drone around a stationary blade . This can be extended to a moving blade by using a slant helix or a quasi helical pattern. This is an area of potential future research interest. 3D Reconstruction of constantly shifting scenes and Tracking & Following vehicles in real time can also be performed using a similar approach. UAVs can also be used to monitor and follow flying vehicles such as helicopters air balloons etc. as the capabilities of commercial quadcopters increase. The calculation of error due to wind and other effects can be propagated to other drones in the vicinity which are affected by the similar natural factors. This can be used to predict corrections when autonomously flying a swarm of drones.

### **6.4 Final Remarks**

Structural Health Monitoring of civil structures is an active area of research. In this dissertation, a novel approach of using drones mounted with cameras to monitor civil structures is proposed. A prototype is implemented by using commercial, easily available software and the experimental simulations conducted exhibit that such an approach is not only feasible but also shows promising initial results.

# Appendix A

## Abbreviations

| <b>Short Term</b> | <b>Expanded Term</b>                          |
|-------------------|---|
| SHM               | Structural Health Monitoring                  |
| UAV               | Unmanned Aerial Vehicle                       |
| NDT               | Non Destructive Testing                       |
| GWEC              | Global Wind Energy Council                    |
| AE                | Acoustic Emission                             |
| SFM               | Structure From Motion                         |
| VTOL              | Vertical Take Off From Landing                |
| ISR               | Intelligence, Surveillance and Reconnaissance |
| SLAM              | Simultaneous Localization and Mapping         |
| COTS              | Commercial Off-the-Shelf                      |
| SIFT              | Scale Invariant Feature Transform             |
| IMU               | Inertial Measurement Unit                     |
| FAST              | Features from Accelerated Segment Test        |
| 2D                | Two Dimensional                               |
| 3D                | Three Dimensional                             |
| GPS               | Global Positioning System                     |



# Appendix B

## DJI Phantom 2 Vision Plus

### Specifications

|                                |  |
|--------------------------------|--|
| <b>Battery</b>                 | 5200mAh LiPo Battery                   |
| <b>Max. Flight Speed</b>       | 15m/s                                  |
| <b>Gimbal</b>                  | Upto 90 °                              |
| <b>Camera</b>                  | 14MP, 4384x3288                        |
| <b>Video Recording</b>         | 1080p & 720p                           |
| <b>Controller Battery</b>      | 3.7V, 2000mAh                          |
| <b>Range Extender Distance</b> | 500-700m                               |
| <b>DJI Vision App</b>          | iOS 6.1 or above, Android 4.0 or above |

# Bibliography

- [Manwell2009] J. Manwell, J. McGowan and A. Rogers, “ Wind energy explained -2nd edition” , Chichester, England, John Wiley & Sons, Dec 2009.
- [Crabtree2014] C. J. Crabtree, D. Zappalá and P. J Tavner, “Survey of Commercially Available Condition Monitoring Systems for Wind Turbines”, *In Proceedings of the Durham University School of Engineering and Computing Sciences and the SUPER-GEN Wind Energy Technologies Consortium*, England, United Kingdom, May 2014.
- [Veers2003] P. Veers, T. Ashwill, H. Sutherland, D. Laird, D. Lobitz, D. Griffin, J. Mandell, W. Musial, K. Jackson, M. Zuteck, A. Miravete, S. Tsai and J. Richmond, “Trends in the Design, Manufacture and Evaluation of Wind Turbine Blades”, *Wind Energy*, vol. 6, no. 3, pp. 245-259, Sep 2003.
- [Hansen2008] M.O.L. Hansen, “Aerodynamics of wind turbines - Second Edition”, Sterling, VA, Earthscan, Dec 2008.
- [GeneralElectricPower2015] General Electric Power, “What is Wind Energy? GE Renewable Energy”, Available at: <https://renewables.gepower.com/wind-energy/overview/wind101.html>, Accessed: 16Aug2015.
- [GWEC15] Global Wind Energy Council, “Global Status Overview”, Available at: <http://www.gwec.net/global-figures/wind-energy-global-status/>, Accessed: 15Aug2015.

- [Eriksson2008] S. Eriksson, H. Bernhoff and M. Leijon, "Evaluation of different turbine concepts for wind power", *Renewable and Sustainable Energy Reviews - Elsevier*, vol. 12, no. 5, pp. 1419-1434, Jun 2008.
- [Adaramola2011] M. Adaramola and P. Krogstad, "Experimental investigation of wake effects on wind turbine performance", *Renewable Energy-Elsevier*, vol. 36, no. 8, pp. 2078-2086, Aug 2011.
- [Ghoshal2000] A. Ghoshal, M. Sundaresan, M. Schulz and P. Frank Pai, "Structural health monitoring techniques for wind turbine blades", *Journal of Wind Engineering and Industrial Aerodynamics - Elseviers*, vol. 85, no. 3, pp. 309-324, Apr 2000.
- [Rumsey2008] Mark A. Rumsey and Joshua A. Paquette, "Structural health monitoring of wind turbine blades", *Smart Sensor Phenomena, Technology, Networks, and Systems -SPIE Digital Library*, vol. 9439, pp.1-8, Apr 2008.
- [WindMeasurementInternational2015] Wind Measurement International 2015, "Wind Turbines", Available at: <http://www.windmeasurementinternational.com/wind-turbines/om-turbines.php> Accessed: 16Aug2015.
- [Hameed2009] Z. Hameed, Y. Hong, Y. Cho, S. Ahn and C. Song, "Condition monitoring and fault detection of wind turbines and related algorithms: A review", *Renewable and Sustainable Energy Reviews - Elsevier*, vol. 13, no. 1, pp. 1-39, Jan 2009.
- [Smead2014] K. Smead, "Top 10 Wind Energy Suppliers", *Energy Digital*, pp. 41-47, Nov 2014.
- [Schubel2013] P.J. Schubel, R.J. Crossley, E.K.G. Boateng, J.R. Hutchinson, "Review of structural health and cure monitoring techniques for large wind turbine blades", *Renewable Energy - Elsevier*, vol. 51, pp. 113-123, Oct 2012.
- [Rabiei2013] M. Rabiei and M. Modarres, "Quantitative methods for structural health

- management using in situ acoustic emission monitoring”, *International Journal of Fatigue - Elsevier*, vol. 49, pp. 81-89, Apr 2013.
- [Bouzid2015] O. Bouzid, G. Tian, K. Cumanan and D. Moore, “Structural Health Monitoring of Wind Turbine Blades: Acoustic Source Localization Using Wireless Sensor Networks”, *Journal of Sensors - Hindawi*, pp. 1-11, Dec 2015.
- [Grosse2008] C. Grosse and M. Ohtsu, “Acoustic emission testing”, Springer, Berlin, 2008.
- [Adams2011] D. Adams, J. White, M. Rumsey and C. Farrar, “Structural health monitoring of wind turbines: method and application to a HAWT”, *Wind Energy*, vol. 14, no. 4, pp. 603-623, May 2011.
- [Dam2015] J. V. Dam, L. J. Bond, “Acoustic emission monitoring of wind turbine blades”, *Smart Materials and Nondestructive Evaluation for Energy Systems- SPIE*, pp.1-8, Mar 2015.
- [Moradi2015] M. Moradi, S. Sivoththaman, “MEMS Multisensor Intelligent Damage Detection for Wind Turbines”, *Sensors Journal - IEEE*, vol.15, no.3, pp.1437 - 1444, Mar 2015.
- [MHWF2015] Michellehenry.fr, “Wind farm - ESL Resources”, Available at: <http://www.michellehenry.fr/windfarm.htm> Accessed: 16Aug2015.
- [DNVGL2015] DNV GL, “Third generation wind power - DNV GL”, Available at: <https://www.dnvgl.com/technology-innovation/broader-view/electrifying-the-future/third-generation-wind-power.html> Accessed: 16Aug2015.
- [Yang2010] W. Yang, P.J. Tavner, C.J. Crabtree and M. Wilkinson, “Cost-Effective Condition Monitoring for Wind Turbines”, *IEEE Transactions on Industrial Electronics*, vol.57, no.1, pp.263-271, Jan 2010.

- [Oh2014] K. Y. Oh, J. K. Lee, L.Y. Park, J.S. Lee, B. I. Epureanu, “Blade health monitoring and diagnosis method to enhance operational safety of wind turbine”, *In Proceedings of the IEEE Conference on Precision Electromagnetic Measurements (CPEM 2014)*, pp. 314-315, Rio de Janeiro, Brazil, Aug 2014.
- [Song2014] Y. Song, C. Bowen, A. Kim, A. Nassehi, J. Padget and N. Gathercole, “Virtual Visual Sensors and Their Application in Structural Health Monitoring”, *Structural Health Monitoring SAGE Journals*, vol. 13, no. 3, pp. 251-264, Feb 2014.
- [Márquez2012] F. G. Márquez, A. Tobias, J. P. Pérez and M. Papaelias, “Condition monitoring of wind turbines: Techniques and methods”, *Renewable Energy Elsevier*, vol. 46, pp. 169-178, Oct 2012.
- [LeBlanc2013] B. LeBlanc, C. Niezrecki, P. Avitabile, J. Chen and J. Sherwood, “Damage detection and full surface characterization of a wind turbine blade using three-dimensional digital image correlation”, *Structural Health Monitoring- SAGE Journals*, vol. 12, no. 5-6, pp. 430-439, Nov 2013.
- [Murray2013] C.C. Murray and W. Park, “Incorporating Human Factor Considerations in Unmanned Aerial Vehicle Routing”, *IEEE Transactions on Systems, Man, and Cybernetics Systems*, vol. 43, no. 4, pp. 860-874, Jul 2013.
- [Chadwick2008] R. Chadwick, “Considerations for Use of Aerial Views in Remote Unmanned Ground Vehicle Operations”, *Human Factors and Ergonomics Society Annual Meeting Journal - SAGE Publications*, vol. 52, no. 4, pp. 252-256, Sep 2008.
- [Allen2015] C. Allen, “Quadcopters” Available at:[http://ffden-2.phys.uaf.edu/webproj/212\\_spring\\_2014/Clay\\_Allen/clay\\_allen/works.html](http://ffden-2.phys.uaf.edu/webproj/212_spring_2014/Clay_Allen/clay_allen/works.html) Accessed: 17Aug2015.
- [Gupte2012] S. Gupte, P.I.T Mohandas and J.M. Conrad, “A survey of quadrotor Un-

- manned Aerial Vehicles”, *In Proceedings of the IEEE - Southeastcon 2012*, pp.1-6, Orlando, FL, USA, Mar 2012.
- [Baguley2015] R. Baguley, “Best Drones 2015”, Tom’s Guide, Available at: <http://www.tomsguide.com/us/best-drones,review-2412.html>. Accessed: 17Aug2015.
- [Pri2015] A. Pri, ‘Quadcopters Yaw Roll and Pitch Defined’, Quadcopterflyers.com, Available at: <http://www.quadcopterflyers.com/2015/02/quadcopters-yaw-roll-and-pitch-defined.html>, Accessed: 17Aug2015.
- [TopTenReviews2015] , “The Best RC Drones of 2015 — Top Ten Reviews”, Available at: <http://rc-drones-review.toptenreviews.com/>. Accessed: 17Aug2015.
- [Hoffman2007] G. Hoffmann, H. Huang, S. Waslander and C. Tomlin, “Quadrotor Helicopter Flight Dynamics and Control: Theory and Experiment”, *AIAA Guidance - Navigation and Control Conference and Exhibit*, South Carolina, USA, Aug 2007.
- [Floreano2015] D. Floreano and R. Wood, “Science, technology and the future of small autonomous drones”, *Nature Journals*, vol. 521, no. 7553, pp. 460-466, Mar 2015.
- [Mellinger2011] D. Mellinger, N. Michael, M. Shomin and V. Kumar, “Recent Advances in Quadrotor Capabilities”, *In Proceedings of the IEEE International Conference on Robotics and Automation*, pp. 2964-2965, Shanghai, China, Aug 2011.
- [Chen2013] M.Y. Chen, D.H. Edwards, E.L Boehmer, N.M. Eller, J.T. Slack, C.R. Speck, C.M. Brown, H.G. Williams, S.H. Wilson, C.S. Gillum, G.C. Lewin, M.S. Sherriff, G.T. Garner, “Designing a spatially aware and autonomous quadcopter”, *In Proceedings of the IEEE Conference on Systems and Information Engineering Design Symposium (SIEDS 2013)*, pp.213-218, Charlottesville, USA, Apr 2013.
- [Chirtel2015] E. Chirtel, R. Knoll, C. Le, B. Mason, N. Peck, J. Robarge, G.C. Lewin, “Designing a spatially aware, autonomous quadcopter using the android con-

- trol sensor system”, *In Proceedings of the IEEE Systems and Information Engineering Design Symposium (SIEDS 2015)*, pp.35-40, Virginia, USA, Apr 2015.
- [Guimaraes2012] J.P.F. Guimaraes, T.L. Laura, A.S. Sanca, A.N Schildt, M.S de-Deus, P.J Alsina, A.T da-Silva, A.A.D Medeiros,, “Fully Autonomous Quadrotor: A Testbed Platform for Aerial Robotics Tasks”, *In Proceedings of the IEEE Brazilian Robotics and Latin American Robotics Symposium (SBR-LARS 2012)*, pp.68-73, Fortaleza, Brazil, Oct 2012.
- [Jang2007] J. S. Jang, D. Liccardo, “Small UAV Automation Using MEMS”, *IEEE Aerospace and Electronic Systems Magazine*, vol.22, no.5, pp.30-34, May 2007.
- [Bluteau2006] B. Bluteau, R. Briand, O. Patrouix, “Design and Control of an Outdoor Autonomous Quadrotor powered by a four strokes RC engine”, *In Proceedings of the 32nd Annual IEEE Conference on Industrial Electronics (IECON 2006)*, pp.4136-4240, Paris, France, Nov 2006.
- [Wilson2014] R. L. Wilson, “Ethical issues with use of Drone aircraft”, *In proceedings of the 2014 IEEE International Symposium on Ethics in Science, Technology and Engineering*, pp.1-4, Chicago, IL, USA, May 2014.
- [Ma’sum2013] M. A. Ma’sum, G. Jati, M.K. Arrofi, A. Wibowo, P. Mursanto, W. Jatmiko, “Autonomous quadcopter swarm robots for object localization and tracking”, *In Proceedings of the 2013 IEEE International Symposium on Micro-NanoMechatronics and Human Science (MHS 2013)*, pp.1-6, Nagoya, Japan, Nov 2013.
- [Lugo2014] J. Lugo and A. Zell, “Framework for autonomous onboard navigation with the AR-Drone”, *In Proceedings of the IEEE International Conference on Unmanned Aircraft Systems (ICUAS 2013)*, pp.575-583, Atlanta, GA, USA, May 2013.
- [Achtelik2009] M. Achtelik, T. Zhang, K. Kuhnlenz, and M. Buss, “Visual tracking and control of a quadcopter using a stereo camera system and inertial sensors”, *In Proceed-*

- ings of the IEEE International Conference on Mechatronics and Automation (ICMA 2009)*, pp. 2863-2869, Changchun, China, Aug 2009.
- [Mondragón2011] I.F Mondragón, P. Campoy, M. A. Olivares-Mendez, and C. Martinez, “3D Object following based on visual information for Unmanned Aerial Vehicles”, *In Proceedings of the IEEE IX Latin American and IEEE Colombian Conference on Automatic Control and Industry Applications Robotics Symposium (LARC 2011)*, pp.1-7, Bogota, D.C Columbia, USA, Oct 2011.
- [Hamel2007] T. Hamel and R. Mahony, “Image based visual servo control for a class of aerial robotic systems”, *Automatica - Elsevier*, vol. 43, no. 11, pp. 1975-1983, Nov 2007.
- [Olivares-Mendez2011] Olivares-Mendez, A. Miguel, I. Mondragón, C. Cervera, L.M Pascual and C. Martinez, “Aerial object following using visual fuzzy servoing”, *In Proceedings of the 1st Workshop on Research, Development and Education on Unmanned Aerial Systems (RED-UAS 2011)*, pp. 61-70, Seville, Spain, Dec 2011.
- [Guenard2008] N. Guenard, T. Hamel, R. Mahony, “A practical Visual Servo Control for a Unmanned Aerial Vehicle”, *IEEE Transactions on Robotics*, vol.24, no.2, pp.331-340, Apr 2008.
- [Golightly2005] I. Golightly, D. Jones, “Visual control of an unmanned aerial vehicle for power line inspection”, *In Proceedings of the IEEE 12th International Conference on Advanced Robotics (ICAR '05)*, pp.288-295, Seattle, WA, USA, Jul 2005.
- [Szeliski2011] R. Szeliski, “Computer vision”, London, Springer, 2011.
- [Tomasi1992] C. Tomasi and T. Kanade, “Shape and motion from image streams under orthography: A factorization method”, *International Journal of Computer Vision*, vol.9, no.2, pp.137-154, Nov 1992.
- [Snavely2008] N. Snavely, S. M. Seitz, R. Szeliski, “Modeling the World from Internet



- Photo Collections”, *International Journal of Computer Vision*, vol. 80, no. 2, pp. 189-210, Nov2008.
- [Furukawa2009] Y. Furukawa, B. Curless, S. M. Seitz, R. Szeliski, “Reconstructing building interiors from images”, *In Proceedings of the 12th IEEE International Conference on Computer Vision*, pp.80-87, Kyoto, Japan, Oct 2009.
- [Furukawa2010] Y. Furukawa and J. Ponce, “Accurate, Dense, and Robust Multiview Stereopsis”, *IEEE Transactions on Pattern Analysis and Machine Intelligence*, vol. 32, no. 8, pp. 1362-1376, Aug 2010.
- [Lowe1999] D.G. Lowe, “Object recognition from local scale-invariant features”, *In Proceedings of the Seventh IEEE International Conference on Computer Vision*, vol.2, pp.1150-1157, Kerkyra, Greece, Sep 1999.
- [Goldberg2002] S.B. Goldberg, M.W. Maimone, L. Matthies, “Stereo vision and rover navigation software for planetary exploration ”, *In Proceedings of the IEEE Aerospace Conference 2002*, vol.5, pp.2025-2036, Big Sky, Montana, USA, Mar 2002.
- [NI2015] Zone.ni.com, “Parts of a Stereo Vision System - NI Vision 2012 Concepts Help - National Instrument”, Available at: <http://zone.ni.com/reference/en-XX/help/372916M-01/nivisionconcepts dita/guid-cb42607e-f256-40f5-ab6e-28ec3a33bcda/>. Accessed: 23Aug2015.
- [Rosten2006] E. Rosten, and T. Drummond, “Machine learning for high-speed corner detection”, *Computer VisionECCV*, pp. 430-443. Springer , Berlin, Heidelberg, 2006.
- [Westoby2012] M. Westoby, J. Brasington, N. Glasser, M. Hambrey and J. Reynolds, “Structure-from-Motion photogrammetry: A low-cost, effective tool for geoscience applications”, *Geomorphology -Elsevier*, vol. 179, pp. 300-314, Dec 2012.
- [Ligas2011] M. Ligas and P. Banasik, “Conversion between Cartesian and geodetic coor-

dinates on a rotational ellipsoid by solving a system of nonlinear equations”, *Geodesy and Cartography -Elsevier* , vol. 60, no. 2, Oct 2011.

[Wu2011] C. Wu, “VisualSFM : A Visual Structure from Motion System”, Available at: <http://ccwu.me/vsfm/>, Accessed:25Aug2015.

[Jancosek2011] M. Jancosek, T. Pajdla, “Multi-view reconstruction preserving weakly-supported surfaces”, *In Proceedings of the 2011 IEEE Conference on Computer Vision and Pattern Recognition (CVPR 2011)*, pp.3121-3128, Colorado Springs, USA, Jun 2011.

[Layton2015] J. Layton, “Wind Turbine Output”, HowStuffWorks, Available at: <http://science.howstuffworks.com/environmental/green-science/wind-power4.htm>, Accessed: 26Aug2015.

[OpenCV2015] Docs.opencv.org, “FAST Algorithm for Corner Detection OpenCV 3.0.0-dev documentation”, Available at: [http://docs.opencv.org/3.0-beta/doc/py\\_tutorials/py\\_feature2d/py\\_fast/py\\_fast.html](http://docs.opencv.org/3.0-beta/doc/py_tutorials/py_feature2d/py_fast/py_fast.html), Accessed: 26Aug2015.

[BestQuadcopterReviews2015] Best Quadcopter Reviews, “Best Quadcopter for All Skill Levels - Drone Reviews of 2015”, Available at: <http://www.bestquadcopterreviews.org/>, Accessed: 26Aug2015.